score

D6.2- Exposure and vulnerability assessment methodology report

DATE OF DELIVERY - 30/12/2022

AUTHOR(S):
Rui Figueiredo (RED)
Raymundo Rangel (RED)

This project has received funding from the European Union's Horizon 2020 research and innovation programme under grant agreement No 101003534

DOCUMENT TRACKS DETAILS

Project acronym	SCORE
Project title	Smart Control of the Climate Resilience in European Coastal Cities
Starting date	01.07.2021
Duration	48 months
Call identifier	H2020-LC-CLA-2020-2
Grant Agreement No	101003534

Deliverable Information	
Deliverable number	D6.2
Work package number	WP6
Deliverable title	Exposure and vulnerability assessment methodology report
Lead beneficiary	RED
Author(s)	Rui Figueiredo (RED), Raymundo Rangel (RED)
Due date	31/12/2022
Actual submission date	30/12/2022
Type of deliverable	Report
Dissemination level	Public

VERSION MANAGEMENT

Revision table			
Version	Name	Date	Description
V 0.1	Rui Figueiredo (RED), Raymundo Rangel (RED)	06/12/2022	First draft
V 0.2	Gianbattista Bussi (RED)	07/12/2022	Updated draft internally reviewed
V 0.3	Rui Figueiredo (RED), Raymundo Rangel (RED)	20/12/2022	Updated draft after peer-review from Neslihan Beden (SAMU) and Luís Campos (ENT)
V1.0	Iulia Anton (ATU) Salem Gharbia (ATU)	30/12/2022	Final version

LIST OF ACRONYMS AND ABBREVIATIONS

Acronym / Abbreviation	Meaning / Full text
CCI	Construction Cost Index
CCLL	Coastal City Living Lab
CORINE	Coordination of Information on the Environment
CRS	Coordinate Reference System
DSM	Damage Scanner model
EBA	Ecosystem-Based Approach
EU	European Union
EU-28	European Union with 28-member states
EUROSTAT	European Statistical Office
FEMA	Federal Emergency Management Agency from USA
GDP	Gross domestic product
GIS	Geographic information system
INSYDE	In-depth Synthetic Model for Flood Damage Estimation
IPCC	The Intergovernmental Panel on Climate change
JRC	European Commission's Joint Research Centre
LUISA	Land Use-based Integrated Sustainability Assessment
MERIT	Multi-Error Removed Improved-Terrain
OSM	OpenStreetMap
RAIL	Railway Infrastructure Loss
RAM	Rhine Atlas damage model
SCORE	Smart Control of the Climate Resilience in European Coastal Cities
SERA	Seismology and Earthquake Engineering Research Infrastructure Alliance for Europe
USA	United States of America
WP	Work Package

BACKGROUND: ABOUT THE SCORE PROJECT

SCORE is a four-year EU-funded project aiming to increase climate resilience in European coastal cities.

The intensification of extreme weather events, coastal erosion and sea-level rise are major challenges to be urgently addressed by European coastal cities. The science behind these disruptive phenomena is complex, and advancing climate resilience requires progress in data acquisition, forecasting, and understanding of the potential risks and impacts for real-scenario interventions. The Ecosystem-Based Approach (EBA) supported by smart technologies has potential to increase climate resilience of European coastal cities; however, it is not yet adequately understood and coordinated at European level.

SCORE outlines a co-creation strategy, developed via a network of 10 coastal city 'living labs' (CCLLs), to rapidly, equitably and sustainably enhance coastal city climate resilience through EBAs and sophisticated digital technologies.

The 10 coastal city living labs involved in the project are: Sligo and Dublin, Ireland; Barcelona/Vilanova i la Geltrú, Benidorm and Basque Country, Spain; Oeiras, Portugal; Massa, Italy; Piran, Slovenia; Gdansk, Poland; Samsun, Turkey.

SCORE will establish an integrated coastal zone management framework for strengthening EBA and smart coastal city policies, creating European leadership in coastal city climate change adaptation in line with The Paris Agreement. It will provide innovative platforms to empower stakeholders' deployment of EBAs to increase climate resilience, business opportunities and financial sustainability of coastal cities.

The SCORE interdisciplinary team consists of 28 world-leading organisations from academia, local authorities, RPOs, and SMEs encompassing a wide range of skills including environmental science and policy, climate modelling, citizen and social science, data management, coastal management and engineering, security and technological aspects of smart sensing research.

EXECUTIVE SUMMARY

In the context of the project activities of WP6, entitled "Strategies to increase the financial resilience of coastal cities", the aim of this document is to report on the development of the exposure models for the Massa, Oarsoaldea and Vilanova i la Geltrú CCLLs, and the methodological approaches to assess their vulnerabilities to flooding.

The developed exposure datasets and vulnerability functions will subsequently be used to perform quantitative risk assessments for these three CCLLs through a flood risk model.

This document first provides a brief review of the state of the art and describes the sources of information and the procedures to create the exposure models for the following asset categories:

- buildings;
- population;
- road and railway networks.

Subsequently, a brief review of the state of the art on the vulnerability modelling for the different asset types is provided, followed by a description of the vulnerability assessment procedures adopted for the purpose of the SCORE project.

It is important to emphasize the value of participation and contact with each one of the frontrunner CCLL and the contribution of data and information during the process of creating the exposure models.

This report is accompanied by the demonstrator D6.3 "Exposure database and vulnerability curves for the frontrunners CCLLs".

LINKS WITH OTHER PROJECT ACTIVITIES

The present deliverable (D6.2), together with the corresponding exposure datasets and flood vulnerability functions (D6.3), were developed in the context of WP6's Task 6.2. These outputs will be used in the development of Task 6.3, where quantitative risk assessments will be performed for the CCLLs based on exposure, vulnerability and hazard data. Regarding the latter, there is therefore a further linkage with WP3's deliverable D3.7 - "Package of short-term hazard modelling", which together with the proposed exposure models and vulnerability assessment methodologies of the present D6.2, will serve to produce the results concerning D6.4 "Residual risk assessment report for the frontrunner CCLLs". This task will also include the assessment of residual risk after the implementation of ecosystem-based approaches (EBA) for climate change adaptation, thus linking with WP7 activities. The development of the exposure models was linked to the previous activity from WP2 "CCLL questionnaires", where the first information on the elements and exposure characteristics of the CCLL frontrunners was delivered. Another activity related with the development of the exposure models was the definition of the study areas provided by the CCLLs with the support of WP3.

TABLE OF CONTENT

INDEX OF FIGURES

INDEX OF TABLES

1. INTRODUCTION

Coastal cities, due to their geographic location, are particularly exposed to hydro-meteorological and climate-related natural hazards. The SCORE project, within its various activities, aims to provide information and experience to take steps towards a better understanding of how to mitigate the effects of extreme events in European coastal cities, which are generally increasing in frequency due to the effects of climate change. The analysis of exposed assets and their vulnerability characteristics are key tools to understand the spatial distribution of their most important elements and assets of interest, and provide invaluable information to support the development of risk assessments and risk management activities for different scenarios.

Within the SCORE project, WP6 is responsible for the development of strategies for the achievement of financial sustainability within an integrated coastal zone management framework. To achieve this, a series of modelling and risk assessment activities are required, which include the development of exposure models and vulnerability assessment functions for WP6's three frontrunner CCLLs: Massa (Italy), Oarsoaldea (Spain) and Vilanova i la Geltrú (Spain).

In this context, the present document, entitled "Exposure and vulnerability assessment methodology report", provides exposure and vulnerability information, analysis and specific data for these three CCLLs. After processing available data from local information sources for each CCLL, as well as other larger-scale data for the relevant asset types, exposure datasets were generated for selected study areas within the CCLLs. Flood vulnerability functions were developed based on available models that were considered more suitable for this application case. The outputs of this deliverable will serve as the input for the subsequent Task 6.3, where quantitative risk assessments for different scenarios will be carried out.

2. EXPOSURE

Exposure assessment has a key role in catastrophe risk modelling. This activity encompasses the estimation of the amount and/or value of assets of different types that can potentially be affected in a given region of interest, the key features that determine their vulnerability to a natural hazard, and their geographical distribution (e.g., De Bono & Mora, 2014). In fact, the location of exposed assets is required to perform quantitative risk assessments, where that information is combined with the spatially-distributed hazard component (e.g., probabilities of flood water depths being exceeded at different locations within a city). Therefore, exposure datasets are, by definition, geospatial datasets, i.e., digital maps where the exposure information is associated to spatial coordinates. This section describes the modelling activities carried out to develop consistent exposure dataset comprising various types of exposed assets for WP6's three frontrunner CCLLs, i.e., Massa, Oarsoaldea, and Vilanova i la Geltrú.

2.1. Study areas

The exposure models will subsequently be used for performing quantitative risk assessments, and are therefore developed for areas where the hazard will also be assessed. Such areas were proposed by the CCLLs and defined taking into account flood hazard modelling requirements and limitations as specified by the hazard modelling team of the SCORE project (included in WP3). The study areas for the exposure models cover the hazard-modelling areas located within the CCLLs' administrative boundaries and are shown in Figures 1-3.

Figure 1: Massa CCLL study area (CRS – EPSG:3035).

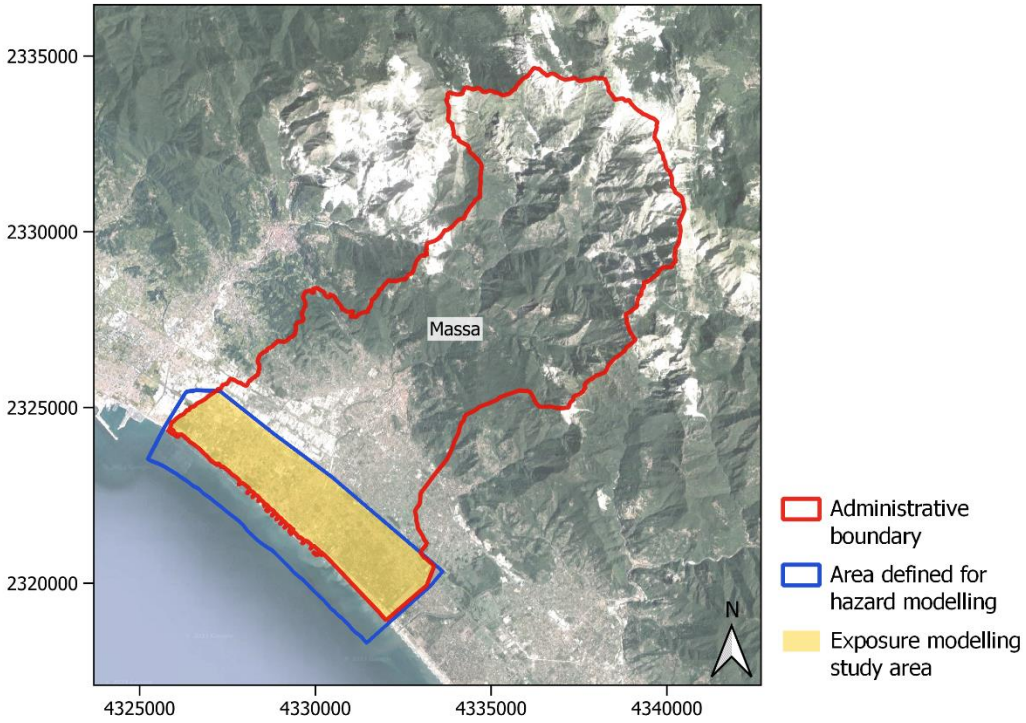

Figure 2: Oarsoaldea CCLL study area (CRS – EPSG:3035).

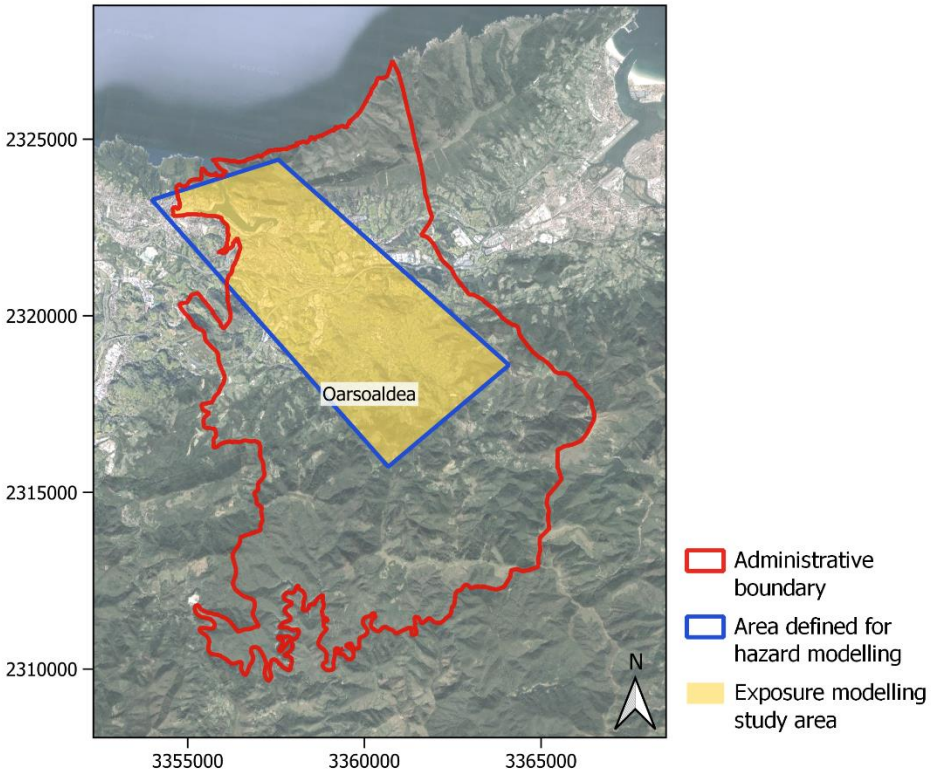

Figure 3: Vilanova i la Geltrú CCLL study area (CRS – EPSG:3035).

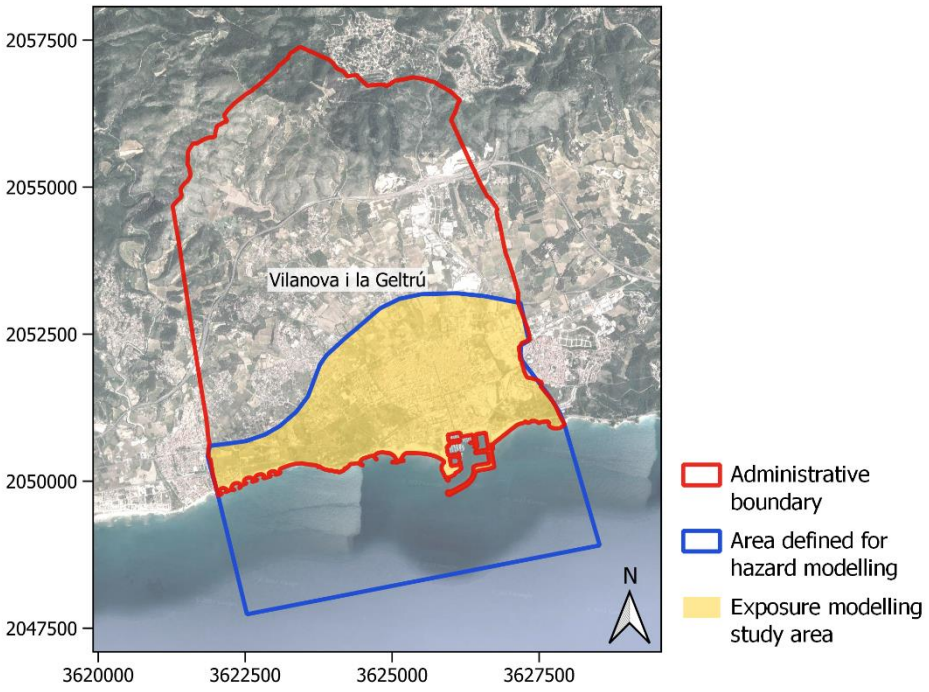

2.2. Buildings

In the development of natural hazard quantitative risk assessment models for large areas, such as municipalities, it is seldom possible to use exposure datasets with all the necessary information about every single building therein. Naturally, from a modelling viewpoint this would be the optimal situation, as it would essentially mean that quantitative risk estimates could be obtained building by building, thus reducing significantly the uncertainty stemming from exposure assessment. However, in most situations, geospatial databases with complete and accurate building-by-building information that are readily available for natural hazard risk modelling purposes simply do not exist. On the other hand, developing such datasets can entail various difficulties related, for example, with limited availability of resources or privacy issues, among others (Dell'Acqua, et al.al, 2013).

In light of this, the development of exposure datasets of buildings for large areas typically requires a modelling effort involving the spatial disaggregation of data that exists at coarser spatial resolutions, i.e., a top-down approach. For example, in the case of residential buildings, national censuses are commonly used as a reliable source of information, but these data are typically available at administrative-unit resolution, such as parish- or municipality-level. The low spatial resolution at which such data are available is not compatible with the resolution that is necessary to accurately model risk. In fact, hazards are usually modelled in grids with higher spatial resolutions, resulting in a mismatch between hazard and census data. In order to resolve this, adequate spatial disaggregation techniques need to be employed. As an example, for residential buildings, the spatial distribution of population has often been used to distribute building data within large regions where building locations are not known or cannot be readily obtained (Silva, et al., 2015).

It is important to highlight that the spatial resolution of a building exposure model should be defined taking into account the properties of the peril for which a risk assessment is to be performed. In fact, losses and risk estimated for events with large, smooth and regularly-shaped footprints such as earthquakes are less sensitive to the resolution of the exposure model than events with narrower and more irregular footprints, such as floods (Chen, et al., 2004).

As an example, while a gridded exposure model with a spatial resolution of 0.04° (approximately 4.5 km at the equator) is considered suitable for the assessment of seismic risk (Paul, Silva, & Amo-Oduro, 2022), this has been shown to be sub-optimal in the case of floods, where higher spatial resolutions are required (Figueiredo & Martina, 2016)

As previously mentioned, obtaining all the required information about every individual building in a large region is not practicable. Nevertheless, for specific limited areas such as municipalities it is sometimes possible to obtain building vector data sets containing some of the needed building attributes, such as their spatial location, geometries (e.g., footprints), and/or possibly other properties (e.g., building use). Still, such datasets generally cannot be directly used to build an exposure dataset because they miss information that is required for risk modelling purposes. However, if this type of building information is combined with additional data available at coarser resolutions, a high-resolution gridded model can be developed through a combination of top-down and bottom-up modelling approaches (Figueiredo & Martina, 2016). Naturally, in this case, available building-specific data take precedence over the coarser resolution data. Also note that the hazard model that is to be geospatially combined with the exposure model for risk assessment is itself a gridded model, meaning that there would be no particular advantage in developing an object-based exposure model, and no significant loss of information will take place as long has the exposure model has a sufficiently high spatial resolution. In summary, for a model with the scale and purposes of the one being developed in WP6, it is advisable to employ a mixture of building level and administrative level data to produce a gridded exposure database, whose grid size is as small as practically possible but typically larger than a single building footprint.

In the context of the WP6, a quantitative risk assessment will be developed for three frontrunner CCLLs. Therefore, targeted efforts can be carried out to obtain more specific information about the buildings therein, which would be impracticable when working for example at the country level. In this context, the data collection and information obtained for each CCLL are described in Section 2.2.1, as well as the complementary data source that were adopted to derive missing building information when necessary. The following subsections then describe how that information was used to develop exposure models for the three CCLLs.

2.2.1. Data collection

An extensive data identification and collection effort was carried out in order to obtain information on the variables that were considered relevant to characterize the vulnerability of the buildings and estimate their replacement costs. In parallel, building-level data were also requested to the CCLLs. Based on this, different information was obtained for each CCLL, which is described in the following subsection. Note that only information deemed relevant for exposure and risk modelling purposes is reported. Additional data sources were adopted to complement these data, and are described in Section 2.2.1.2.

2.2.1.1. Building-by-building data

Massa

Building data for the Massa CCLL were obtained from GEOscopio[1], the geoportal of Tuscany, Italy. GEOscopio provides access to numerous types of geographical data for the region of Tuscany, among which for buildings. The GEOscopio building geospatial vector data include building footprints, subdivided by volumetric units (which are defined as the portions of buildings with homogeneous heights), and information on their type of use and height, in meters. These data are illustrated in Figure 4. For this CCLL, it was not possible to obtain additional building-specific data of relevance for the present task.

[1] https://www.regione.toscana.it/-/geoscopio

Figure 4: Example of building data obtained for the Massa CCLL (CRS – EPSG:3035).

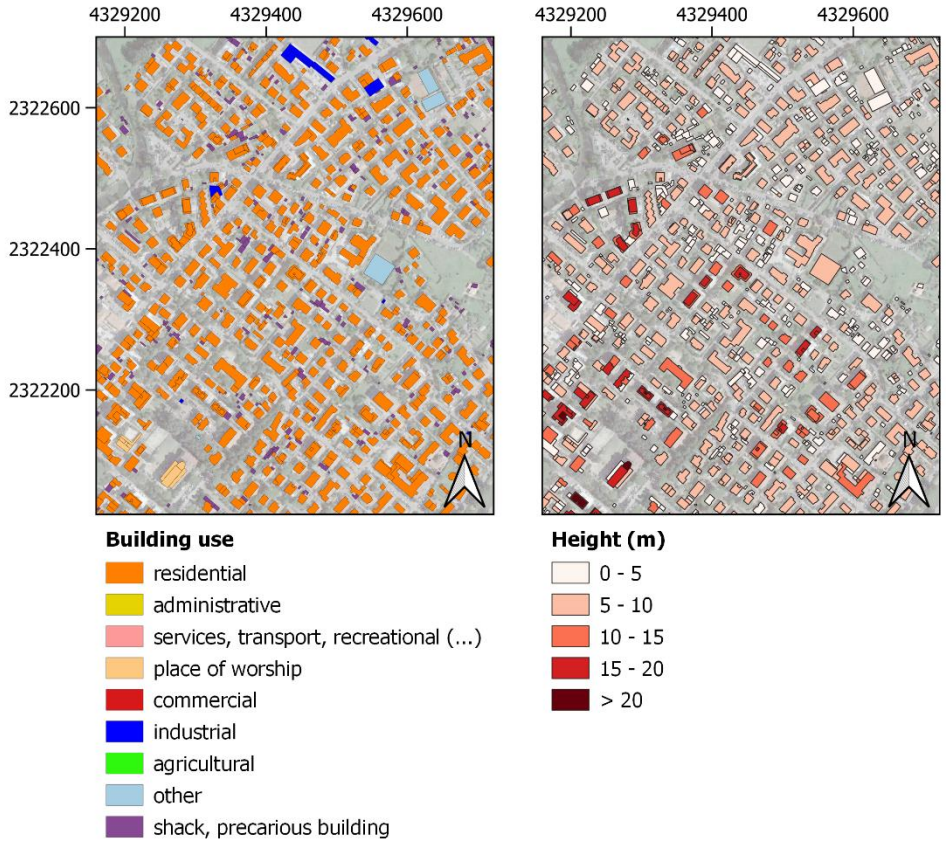

Oarsoaldea

Regarding the Oarsoaldea CCLL, three building-level geospatial vector datasets were collected. A dataset named *ERAIKINAK_EDIFICIOS* was obtained from the Spatial Data Infrastructure of Gipuzkoa[2], a geoportal managed by the Department of Mobility and Planning of the Gipuzkoa province, Basque Country, Spain, and contains the following information: building footprints; two attributes related with the building type (i.e., type and subtype); the attribute *name*, which contains the use type of the building and its activity name (e.g., name of a business, name of a country house, name of a church), albeit in a non-standardized manner and only for approximately 30% of the building polygons located within the Oarsoaldea administrative boundary; and average and maximum height, in meters, for 95% of the building polygons within that area.

The CCLL provided two additional building geospatial datasets for the development of this task. The first, named *BTA_EDI_EDIFICACIONES_A_1E5_ETRS89*, contains footprints for building blocks (i.e., groups of adjacent buildings, rather than individual buildings), a *name* attribute referring to the name of the activity carried out in the building (but only for 5% of the building polygons within the Oarsoaldea administrative boundary), and an attribute named *legend* with a classification of the buildings according to their type. The second building dataset, named *Eraikuntz-score*, contains polygons representing building footprints, as well as information on the buildings' number of storeys above and below ground, and their average and maximum heights in meters. This information is available for around 70% of the building polygons in the dataset; for the remaining ones, only footprints are provided. Based on a visual comparison with aerial imagery, some existing buildings are observed not to be presented in this dataset.

Given that all three datasets contain useful information, they were merged into a single dataset before subsequent modelling steps. In terms of building polygons, the *ERAIKINAK_EDIFICIOS* dataset was used as the reference, as it

[2] https://b5m.gipuzkoa.eus/web5000/en

appears to provide the most accurate and complete representation of existing buildings in the CCLL. The data present in the two other geospatial datasets, described above, were joined onto this dataset through a spatial join operation in a GIS environment.

In order to complement these data, personnel from the CCLL also elaborated a comprehensive document containing textual information on the main constructions materials and presence of basements in Oarsoaldea, aggregated at district and sub-district (i.e., neighbourhood) levels, and images depicting those zones. An example is provided in Figure 5. In order for this information to be applicable in the development of the building exposure model, it was converted into a geospatial dataset. To do this, the areas were first manually mapped onto 75 different polygons in a GIS environment, and the textual information for each area was interpreted and converted into quantities (e.g., "usually with basement" is generally interpreted as 70% of the buildings having basement and 30% having no basement).

Figure 5: Example of information on building materials and presence of basement at aggregated level provided by the Oarsoaldea CCLL.

Detail of San Juan: old town in dark red, modern town in yellow and rural zone in green. GeoEuskadi.

In this district we have three different zones (figure 30): the old town where the buildings are made of masonry and wood and have not basement; the modern part, where we can find houses built in reinforced concrete usually with basement, and industrial buildings made of steel and/or reinforced concrete without basement; the third zone corresponds to the rural zone, where are some houses/farms built in masonry and wood without basement, and a few of reinforced concrete buildings like an school.

Vilanova i la Geltrú

Building data for Vilanova i la Geltrú were obtained from the INSPIRE Services of Cadastral Cartography[3], managed by the General Directorate of Cadastre of Spain. The data comprise two layers: the first (named *A.ES.SDGC.BU.08308.building*) contains building footprint polygons and the use type of the buildings, whereas the second (*A.ES.SDGC.BU.08308.buildingpart*) provides finer-resolution polygons representing building volumes and includes information about the number of storeys above and below ground for each of those volumes. These data are illustrated in Figure 6. Similarly to case of Massa, it was not possible to obtain additional building-specific data of relevance for the Vilanova I la Geltrú CCLL.

[3] http://www.catastro.minhap.gob.es/webinspire/index_eng.html

Figure 6: Example of building data obtained for the Vilanova i la Geltrú CCLL (CRS – EPSG:3035).

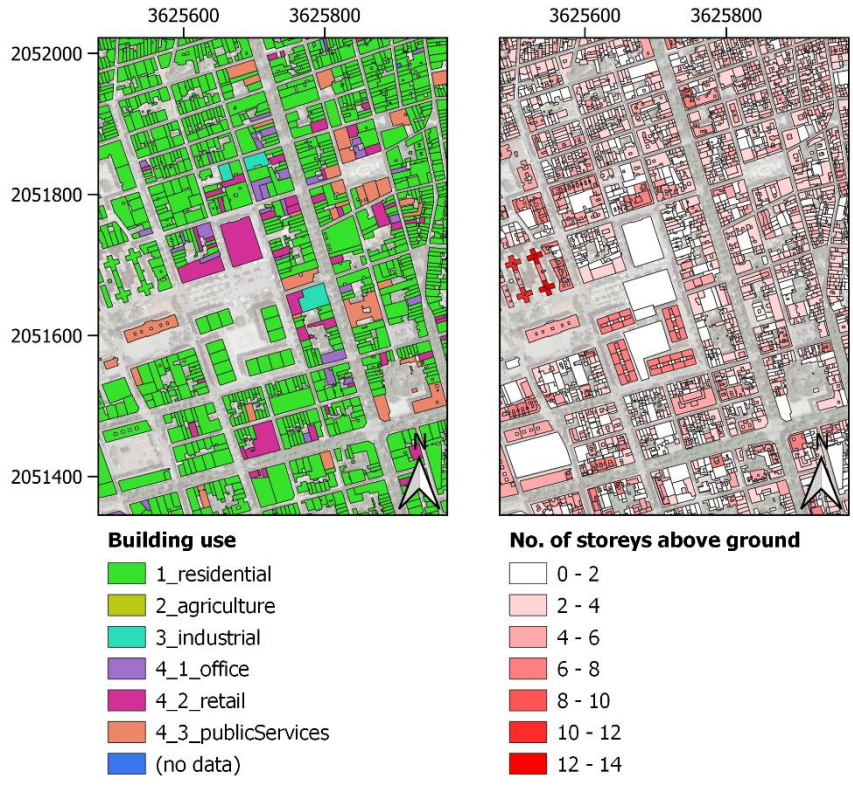

2.2.1.2. Complementary building data

In order to complement the building-specific data described in the previous subsection, which do not contain all the information needed for the development of an exposure model for risk modelling purposes (either because some variables are not provided or because they do not cover all the existing buildings), additional data sources were investigated and are described in this subsection.

Census data

As mentioned previously, national censuses often include some information about buildings that can be useful in the development of exposure models, particularly for residential buildings. Therefore, in this case, national census data relative to the two countries where the three WP6's frontrunner CCLLs are located (Italy and Spain) were analysed. Taking into account the building-specific data that were already previously collected for the three CCLLs, it was found that complementary information of interest could be obtained for the case of Massa, specifically building material types, available from the Italian 2011 general population and housing census[4] at census block level. Census blocks in Italy are portions of land that share similar environmental and socio-economical characteristics; they can be a fraction of a municipality, an entire municipality or they can include more than one municipality, although the latter is relatively rare. For each census block, these data include the number of residential buildings whose main construction materials is masonry, reinforced concrete or others. Figure 7 shows some of the census blocks for the Massa CCLL, superimposed on the building dataset presented in Section 2.2.1.1, illustrating the spatial resolution at which this information is available.

[4] https://www.istat.it/

Figure 7: Example of census blocks for the Massa CCLL, for which residential building information is available (CRS – EPSG:3035).

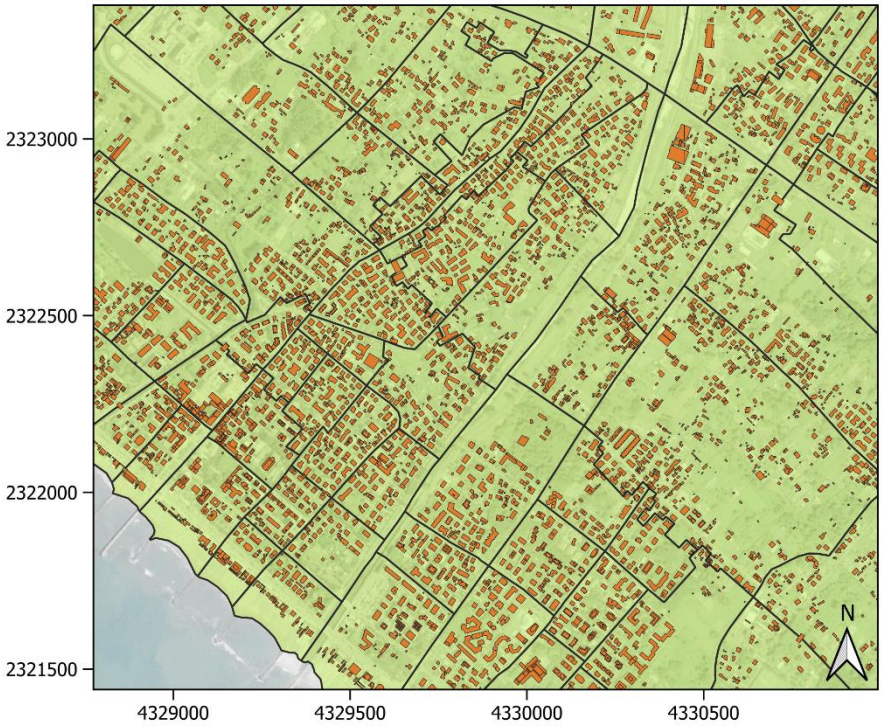

SERA building exposure model

The SERA European building exposure model was also adopted as a complementary data source for the present task. This model, which was developed as part of the Horizon 2020 project SERA (Seismology and Earthquake Engineering Research Infrastructure Alliance for Europe), describes the distribution of residential, commercial and industrial buildings according to certain classes that are relevant to characterize their seismic performance in a consistent manner. The building attributes present in the model include the main construction material, the lateral load resisting system, the number of storeys, the seismic design code level, and the lateral force coefficient used in the seismic design (Crowley, et al., 2020). Because the exposure model developed in the present task is designed for application in the risk assessment of flood-related hazards, certain seismic-specific attributes in the SERA model are not relevant. However, information on construction materials and number of storeys is useful for estimating the flood vulnerability and replacement costs of buildings, as explained further below. The SERA exposure data can be accessed through a GitLab repository[5] and are available in different resolutions depending on the country and building use type. For example, for residential buildings, data for Spain are available at the province level, whereas for Italy they are available at the municipality level. Instead, industrial building data is provided as a grid with a spatial resolution of 30 arc seconds.

2.2.2. Taxonomy

A core feature of an exposure model is the taxonomy used to identify the assets, in this case, the buildings. A building taxonomy can be defined as a classification scheme used to categorize assets according to certain key characteristics that they have in common and that are informative for assessing and differentiating their vulnerability to a given

[5] https://gitlab.seismo.ethz.ch/efehr/esrm20_exposure/

peril. Accordingly, when designing a building taxonomy for a given exposure model, three main aspects should be taken into account:

- The peril, which determines the building properties that it makes sense to include in the exposure model. This is because different hazards cause different types of damage to buildings, and those damages are driven by different building characteristics. As an example, for windstorm risk assessment, information on the roof type would be relevant, whereas for floods that would not be the case, as this feature has no influence on a building's flood vulnerability.
- The building information that can be exploited in vulnerability models for the assessment of losses. In this case, there would be little added value in creating taxonomical classes referring to building properties that, although known to have some influence on the flood vulnerability of a building, cannot be used as inputs for applicable vulnerability models.
- The availability of data. The taxonomy should reflect the data that is actually available and usable for the development of a building exposure model.

Taxonomical classes are also useful to associate appropriate and differentiated replacement costs per area unit (in this case EUR/m^2) to different typologies of buildings.

The building taxonomy for the present task was developed taking into account the above considerations. The taxonomy comprises four main building characteristics that are informative and applicable for the assessment of flood vulnerability, and at the same time available for the three CCLLs: building use (i.e., occupancy type), construction material, presence of basements, and building height in terms of number of storeys. Each of these characteristics is described in the taxonomy by unique string codes, which are presented and described in Table 1. Together, the strings referring to the four building features make up a taxonomical code that will represent a building typology, to which a vulnerability function and a replacement cost can subsequently be associated.

Table 1: Exposure model taxonomy classes, string codes, and descriptions.

Building feature	Code	Description
Use type	RESMIX	Residential / mixed use buildings
	PUBLIC	Public buildings
	INDCOM	Industrial and commercial buildings
	PRTBLD	Buildings belonging to port areas
Material	RC	Reinforced concrete
	MSN	Masonry
	STL	Steel
	OTH*	Other materials
Basement	B	Building has basement(s)
Height	L	1 – 3 storeys
	M	4 – 6 storeys
	H	> 6 storeys

* This class is specific to residential buildings in the Massa municipality, as provided in the Italian census data.

Two examples are provided to illustrate the taxonomy: 1) the taxonomical code for residential buildings in reinforced concrete, with basement, and with 4–6 storeys above ground is RESMIX_RC_B_M; 2) the taxonomical code for industrial buildings in steel, without basement, and with 1–3 storeys above ground is INDCOM_STL_L. Regarding the presented taxonomy, a few specific remarks are warranted. In the case of building use types, the classes were designed to accommodate and harmonize the corresponding data that are available for the three CCLLs, which are significantly heterogeneous. Also, regarding use types, the class PRTBLD (which, in terms of building features and replacement costs, is assumed to be similar to INDCOM) was included because the CCLLs of Oarsoaldea and Vilanova i la Geltrú have important port areas, and it is envisaged that it may useful to differentiate the buildings therein when performing quantitative risk assessments in future project tasks. Lastly, in terms of the building height class, it is noted that this property would not be strictly necessary for the assessment of flood losses and risk, because in the vast majority of cases floods do not affect storeys above the ground floor. Therefore, contrary to other hazards, the actual exposure of buildings to flooding is essentially located at this level, and correspondingly, monetary losses can be quantified for that exposure. However, in the development of the present exposure model, the "number of storeys" class is considered for two reasons: first, the number of storeys is directly related with the total replacement costs of buildings, and this information may be useful to assess relative losses in a certain area (e.g., losses expressed as the fractions of the total replacement costs); and second, including height information may increase the usefulness of the exposure model for assessing risks for hazards other than floods, even if that is not foreseen in the project.

2.2.3. Methodology

This subsection describes how the building data collected for each of the CCLLs was processed and combined to generate exposure models for the respective study areas. The general procedure consisted in assigning building classes for each building polygon, based on the modelling steps described in Section 2.2.3.1, and then aggregating this information into grids with a spatial resolution of 100 m x 100 m. For each CCLL, two building exposure datasets were generated. The first contains, for each grid cell and taxonomical class, the replacement cost of the parts of the buildings considered potentially exposed to flooding, computed as the sum of the product of the footprint areas in each cell by the associated replacement costs per m^2 (described in Section 2.2.3.2). The second dataset contains the total replacement costs of the buildings of each class (i.e., not just the replacement costs of the parts considered potentially exposed to flooding; therefore, computed as the sum of the product of the buildings footprint areas by their number of storeys and their associated replacement costs per m^2).

2.2.3.1. Building properties

Massa

For the Massa CCLL, information on building use types exists at the building level and was found to be complete and to have a good level of accuracy. Therefore, the only required modelling step for this property consisted in establishing the relation between building use raw data (i.e., as provided in the original datasets) and the defined taxonomical classes adopted for the exposure model.

In terms of building materials, no information is available at the building level. For residential buildings, the highest-resolution data for this property is available from census block data, as previously described. These data were spatially disaggregated by performing a random sampling procedure, in order to assign a material to each building polygon of class RESMIX and PUBLIC within the census block, based on the relative frequencies of the buildings of each material present therein. The PUBLIC class was included in the disaggregation procedure as no specific information for this building use type is available. Note that the random sampling procedure is not meant to accurately assign properties on a building-by-building basis (which is not possible, as the information does not exist), but instead to allow for a spatial disaggregation of data available at a much coarser spatial resolution in such a way that the information can be taken advantage of when estimating aggregate losses (i.e., at exposure grid cell and/or municipality level) and risk, which is the objective here.

A similar random sampling procedure was adopted for building polygons belonging to the INDCOM class. In this case, the material distribution was taken from SERA data available for the municipality. The distribution shown in Table 2 was considered.

Table 2: Probabilities of INDCOM building materials for the Massa CCLL, based on SERA data.

Material class	Probability
RC	0.73
MSN	0.05
STL	0.22

Regarding the presence of basements in buildings, no information is available for the Massa CCLL. Based on the inspection of street-level imagery in the study area, 25% of the buildings therein were assumed to have basement, and a random sampling procedure was carried out to spatially distribute this information.

Lastly, information on the number of storeys is also not available for the Massa CCLL. However, height information is provided for the polygons representing different building volumes. Therefore, for buildings belonging to the RESMIX and PUBLIC classes, the relation between building heights and number of storeys presented in Figueiredo & Martina, 2016 was adopted (Table 3). Because this relation is not considered adequate for buildings of the INDCOM class, the distribution of the number of storeys available in the SERA dataset was used for this class (see Table 4), and a random sampling procedure was carried out to spatially disaggregate this information.

Table 3: Adopted correspondence between height intervals and number of storeys.

Height (m)	No. storeys
h ≤ 5.00	1
5.00 < h ≤ 8.80	2
8.80 < h ≤ 12.30	3
12.30 < h ≤ 15.40	4
15.40 < h ≤ 19.30	5
19.30 < h ≤ 22.00	6
22.00 < h ≤ 24.70	7
h > 24.70	8+

Table 4: Probabilities of INDCOM building materials for the Massa CCLL, based on SERA data.

No. storeys	Probability
1	0.86
2	0.09
3	0.03
4	0.02

Oarsoaldea

For Oarsoaldea, building use classes were assigned in a two-step process. First, relevant information found in the three provided datasets were combined, more specifically building types (e.g., generic building, industrial building) and the names of the activities associated with the buildings, when available. Regarding the latter, a semi-automated procedure was developed to associate certain commonly found descriptive keywords to building use classes in the taxonomy model. For the cases where this was not possible, the correspondence was established manually. Subsequently, an extensive manual assessment was carried out, based on a combination of satellite and street-level imagery analysis, both to complement remaining gaps for polygons without any of those data and to correct various instances where the original raw data was found to be inaccurate. Lastly, the PRTBLD class was assigned to buildings located within the Oarsoaldea port area.

Building material information was not available at building polygon level for Oarsoaldea. In this case, the elaboration of building material data aggregated at municipality- and neighbourhood-level provided by the CCLL, described in Section 2.2.1.1, was used, and a random sampling approach analogous to the one described for Massa was adopted to spatially distribute the information within those areas. The same procedure was adopted regarding the presence of basements, although in this case information was already available at polygon-level for a number of buildings. Therefore, the random sampling was used to complement this information for buildings with no data.

The number of storeys was available for approximately 70% of the building polygons, while building height was available for around 95% of polygons. A sanity check of these data was carried out, using satellite and street-level imagery, in order to assess their reliability. As it is not practicable to carry out this type of assessment for all buildings in the municipality, the analysis focused on two types of cases: 1) buildings where the relation between height and number of storeys did not make sense (i.e., tall buildings with a disproportionately low number of storeys and vice-versa), and buildings with very large footprint areas (as in this case a wrong definition of the number of storeys would potentially lead to significant errors in the calculation of the replacement costs for the exposure model). Although the information was generally found to be accurate, numerous instances were detected where the number of storeys was incorrectly defined and were manually corrected.

For buildings of the RESMIX and PUBLIC classes where the height was available but the number of storeys was not, the relation adopted for Massa and shown in Table 3 was used to estimate the latter. Also, analogously to the Massa CCLL case, for the INDCOM and PRTBLD classes the distribution of number of buildings with different number of storeys was estimated based on data from the SERA exposure model and spatially disaggregated.

Vilanova i la Geltrú

Information on building use types for Vilanova i la Geltrú is complete and generally accurate. Therefore, similarly the case of the Massa CCLL, these data were harmonized by establishing a correspondence between the raw data and the adopted taxonomical classes. The PRTBLD class was assigned to buildings in the area of the Vilanova i la Geltrú port.

Regarding building materials, no information exists at the building level, and the highest-resolution data available for use in the present task were obtained from the SERA exposure dataset at province level. Thus, as for the other CCLLs, these data were spatially disaggregated through a random sampling procedure in order to assign a material to each building polygon of class RESMIX and PUBLIC within the study area. In this case, probability distributions conditional on the number of storeys above ground – which in this case are available for all polygons – were adopted (Table 5). By doing this, it is possible to perform the spatial disaggregation in a more accurate manner, as for these types of buildings, materials tend to vary significantly for depending on the number of storeys (e.g., masonry is more common in low-rise than in high-rise buildings). For buildings of class INDCOM, a similar spatial disaggregation procedure was used, although in this case a single probability distribution was adopted (Table 6), as the variability in number of storeys for buildings of this class is much lower and less related with building materials. For the PRTBLD class, based on a visual analysis of the buildings from aerial- and street-level imagery, a probability of 0.50 was considered for RC and MSN buildings.

Table 5: Probabilities of RESMIX and PUBLIC building materials for the Vilanova i la Geltrú CCLL, conditional on the number of storeys, based on SERA data.

No. of storeys	Material class probability	
	RC	MSN
1	0.00	1.00
2	0.18	0.82
3	0.33	0.67
4	0.29	0.71
5	0.25	0.75
6	0.22	0.78
7+	1.00	0.00

Table 6: Probabilities of INDCOM building materials for the Vilanova i la Geltrú CCLL, based on SERA data.

Material class	Probability
RC	0.38
MSN	0.08
STL	0.54

Information on the presence of basements, available for all building polygons, was used to categorize the corresponding taxonomical class.

2.2.3.2. Building replacement costs

The exposure model expresses value in terms of replacement costs that are estimated based both on the taxonomical classes of the buildings, as previously described, and on their location, as replacement costs vary among countries. In order to define unit costs for use in the present task, three main sources of information were investigated. The first is the European Commission's Joint Research Centre (JRC) technical report entitled "Global flood depth-damage functions" (Huizinga, et al., 2017) and its supporting material. This publication provides consistent reconstruction unit costs for residential, commercial and industrial buildings worldwide, which are estimated through statistical regressions developed based on construction cost survey data and GDP per capita data for multiple countries. The second source of information is the previously described SERA dataset, which also provides estimates of replacement unit costs for different building classes and countries. The third source of information is RED's internal database of replacement unit costs for buildings, which has been developed over the years based on multiple sources that include detailed construction cost data for a large number of buildings, construction market survey data, and analyses of technical documentation, reports, and scientific literature.

Note that the developed exposure model is intended to reflect the full replacement costs of the buildings, i.e., both the buildings themselves and their contents. Typically, construction cost data used in the development of exposure models for risk assessment purposes refer only to the former. To address this, both the JRC and SERA documentation – as well as several other sources (de Moel, et al., 2013) – propose that the replacement costs of building contents are expressed as a fraction of the building repair/reconstruction costs. Based on this, Table 7 shows the adopted fractions of replacement costs associated to building and contents; the full replacement cost is obtained by dividing the building-only reconstruction cost by the fraction of the total value that it is assumed to represent for each

building use class. The relative damage estimates provided by building vulnerability functions are applicable to full replacement cost figures based on the assumption that relative damage to building and contents increases proportionately.

Table 7: Fractions of total replacement costs associated with building and contents, depending on the building use class.

	Replacement cost fractions for building use classes	
	RESMIX	INDCOM
Building	0.70	0.40
Contents	0.30	0.60

The reference replacement costs obtained from the different data sources are relative to different years. Therefore, it was necessary to first update them so that they refer to the same year, in this case 2021, and are therefore comparable. This was done using two alternative approaches: 1) by multiplying the original replacement costs by the ratio between the respective country's GDP per capita for 2021 and for the year that the original replacement costs refer to; 2) by multiplying the original replacement costs by the ratio between the respective country's Construction Cost Index (CCI) for 2021 and for the year that the original replacement costs refer to. Both GDP per capita and CCI data for Italy and Spain were obtain from Eurostat[6].

Replacement unit costs are assumed to depend mainly on the building use type and on their main construction material. In order to estimate the unit costs for the various combinations of these two properties, first, baseline values for the RESMIX and INDCOM classes for Italy and Spain were computed based on mean values of the updated replacement costs derived from the different data sources using the two updating methods described above, including contents. The values range from approximately 1,850 EUR/m^2 (RESMIX, Spain) to approximately 2,300 EUR/m^2 (INDCOM, Italy). The baseline values for the PUBLIC class were estimated by applying a multiplying factor of 1.10 to RESMIX unit costs, while the PRTBLD class was assumed to have replacement unit costs similar to those of the INDCOM class. Then, in order to adapt these reference unit costs for building types of different material classes, a multiplier-based approach was adopted, in line with the methodology that is used in all three data sources described above. The multipliers adopted for the different material classes are shown in Table 8.

Table 8: Adopted multipliers to estimate replacement unit costs for buildings belonging to the different material classes present in the exposure model.

Material class	Multiplier
RC	1.00
MSN	0.95
STL	0.95
OTH	1.00

[6] https://ec.europa.eu/eurostat/web/main/data/database

2.2.4. Outputs

Based on the methodological steps described above, geospatial building exposure datasets were developed for the Massa, Oarsoaldea and Vilanova i la Geltrú CCLLs. The datasets are structured in a vector data format comprised of regular grids of polygons with 100 m x 100 m, and are saved as layers of the complete exposure dataset geopackages that are part of D6.3 of the SCORE project. Two building exposure layers are provided, in line with the explanation provided in Section 2.2.2: one referring replacement costs considered exposed to flooding, and the other referring to total replacement costs. The dataset for each CCLL study area has *N*+2 attributes: the *id* attribute contains unique grid cell identification numbers; *N* attributes are titled as each of taxonomical classes that exist in the study area and contain the associated replacement costs; and the *SumRepCost* contains the sum of the replacement costs of all taxonomical classes for each grid cell. Table 9 provides an overview of some of the features and information in the exposure datasets, whereas Figures 8 to 13 present illustrative maps and summary bar plots depicting some of the data on overall estimated replacement costs disaggregated by different taxonomical classes.

Table 9: Summary values of the developed gridded exposure models.

	CCLLs		
	Massa	Oarsoaldea	Vilanova i la Geltrú
No. of grid cells in the study area	1640	3643	1188
No. of grid cells containing buildings	1287	1388	668
No. of taxonomical classes	42	43	37
Total replacement cost (million EUR)	3800.0	12781.6	8641.7

Figure 8: Geographical distribution of replacement costs considered potentially exposed to flooding for the Massa CCLL (CRS – EPSG:3035).

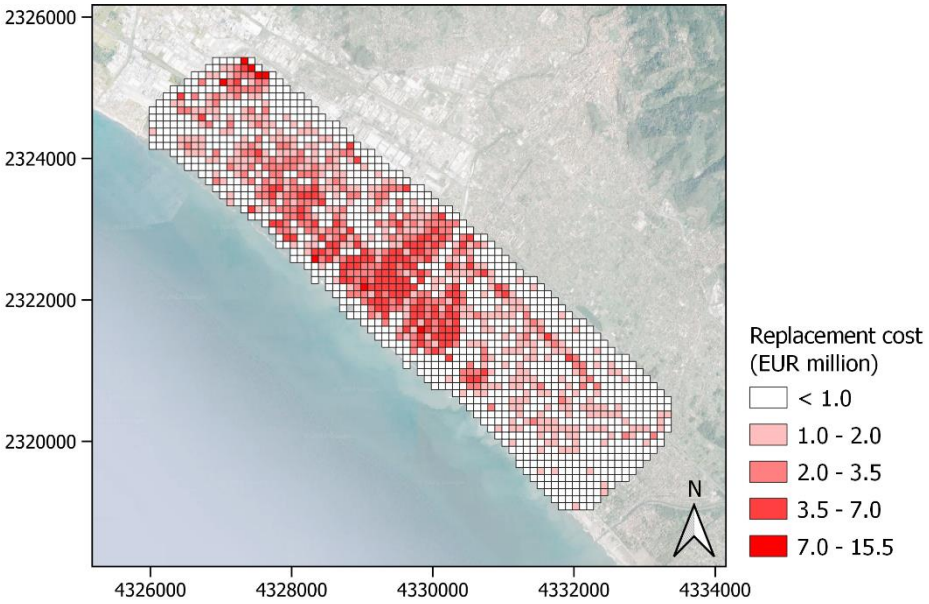

Figure 9: Bar plots of replacement costs considered potentially exposed to flooding for the Massa CCLL, relative to the building use and building material taxonomical classes.

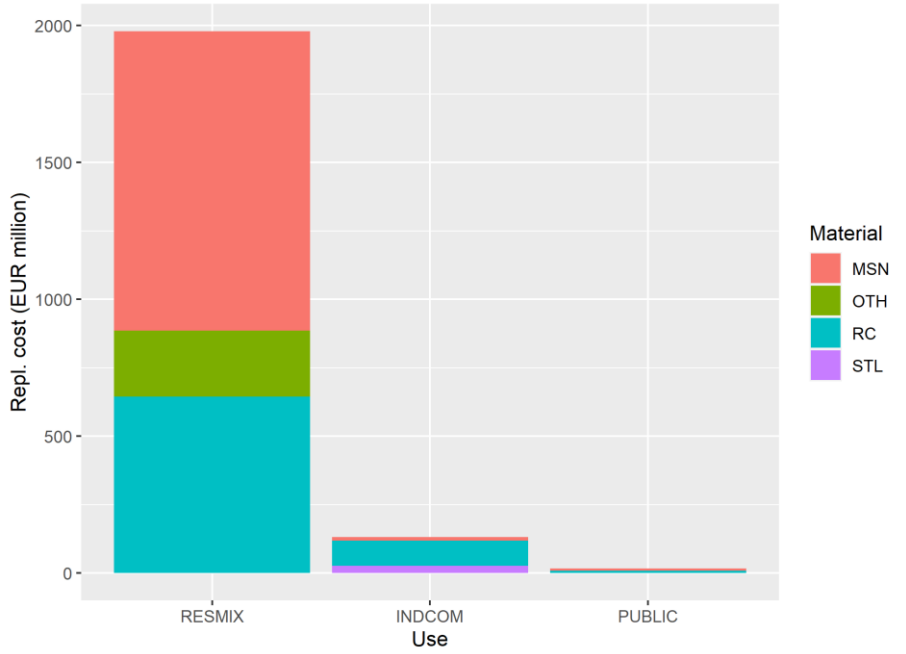

Figure 10: Geographical distribution of replacement costs considered potentially exposed to flooding for the Oarsoaldea CCLL (CRS – EPSG:3035).

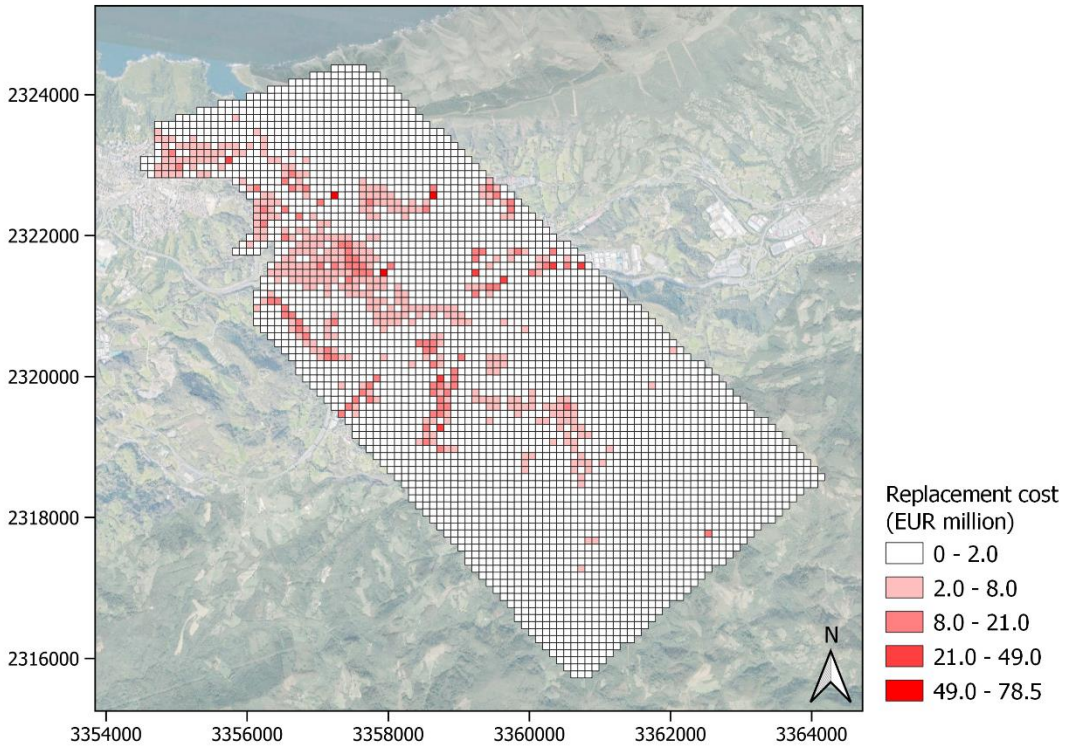

Figure 11: Bar plots of replacement costs considered potentially exposed to flooding for the Oarsoaldea CCLL, relative to the building use and building material taxonomical classes.

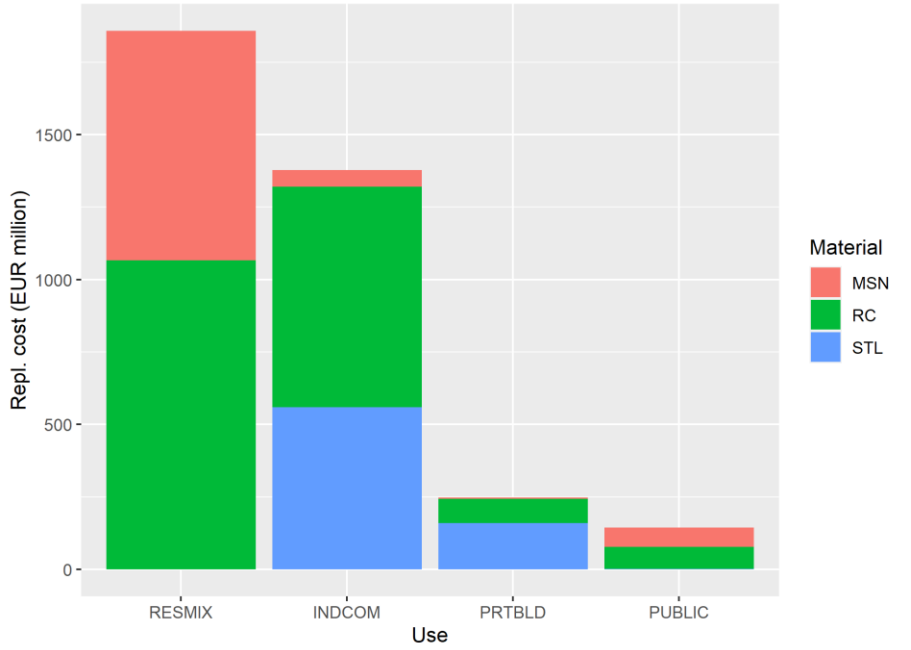

Figure 12: Geographical distribution of replacement costs considered potentially exposed to flooding for the Vilanova i la Geltrú CCLL (CRS – EPSG:3035).

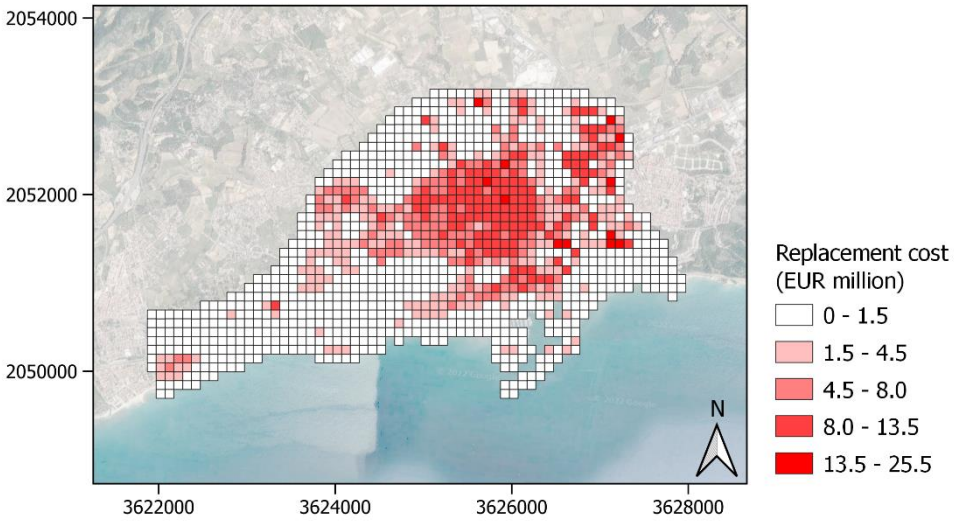

Figure 13: Bar plots of replacement costs considered potentially exposed to flooding for the Vilanova i la Geltrú CCLL, relative to the building use and building material taxonomical classes.

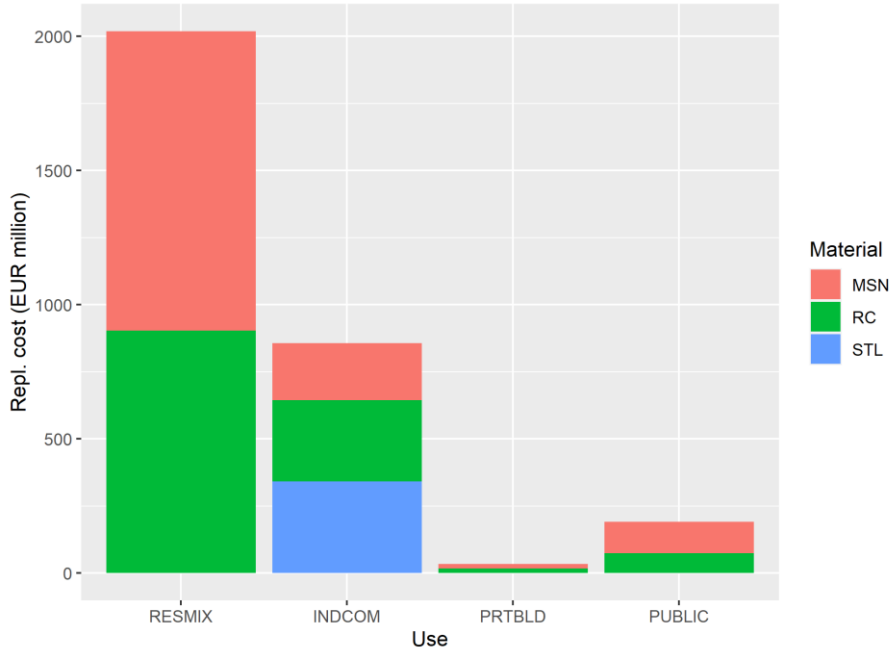

2.3. Population

Population growth, particularly urbanization trends and the associated increased population density, is a driver of increasing vulnerability and natural hazard risk for societies worldwide (Charles, 2007). The growth of population in coastal cities, for instance, raises important concerns about increased human exposure to flood-related hazards, in particularly coastal flooding. Moreover, population also tends to be more vulnerable than other assets of the built environment, such as critical infrastructure or building, to slow-onset climate-related hazards like droughts, heatwaves or cold waves, which can in turn also increase their vulnerability to subsequent hazard types, including flooding. For these reasons, population is among the elements that should be considered in risk assessment processes, where the impact can be quantified in terms of number of affected persons. A reference to this is found in FEMA (2022), where the USA's Federal Emergency Management Agency considers that population exposure can be defined as the number of people determined to be exposed to a hazard. In light of this, exposure datasets for population are provided as part of the present task. The present section describes the associated data collection, methodology, and outputs.

2.3.1. Data collection

The three CCLLs have delivered information related to the population and its features over their municipality area. However, this information is aggregated at municipality level. Therefore, for this task, two sub-municipality population gridded datasets were reviewed in order to derive a higher-resolution exposure dataset: WorldPop[7] and Meta[8] (previously Facebook).

The WorldPop gridded data are provided at a resolution of 100 m x 100 m, whereas the Meta data are available at a higher resolution of 20 m x 20 m. However, the latter was found to not contain a sub-municipality disaggregation of the population information, i.e., within each municipality-level administrative boundary the population density is the same for all grid cells where population is considered to exist. Figure 14 provides an illustrative comparison using

[7] https://www.worldpop.org
[8] https://dataforgood.facebook.com/dfg/tools/high-resolution-population-density-maps

maps of the two datasets for the Vilanova i la Geltrú CCLL. For this reason, the WorldPop dataset was considered more adequate for this task and was adopted.

Figure 14: Comparison of population density for Vilanova i la Geltrú from the Meta (left) and WorldPop (right) gridded population datasets (CRS – EPSG:3035).

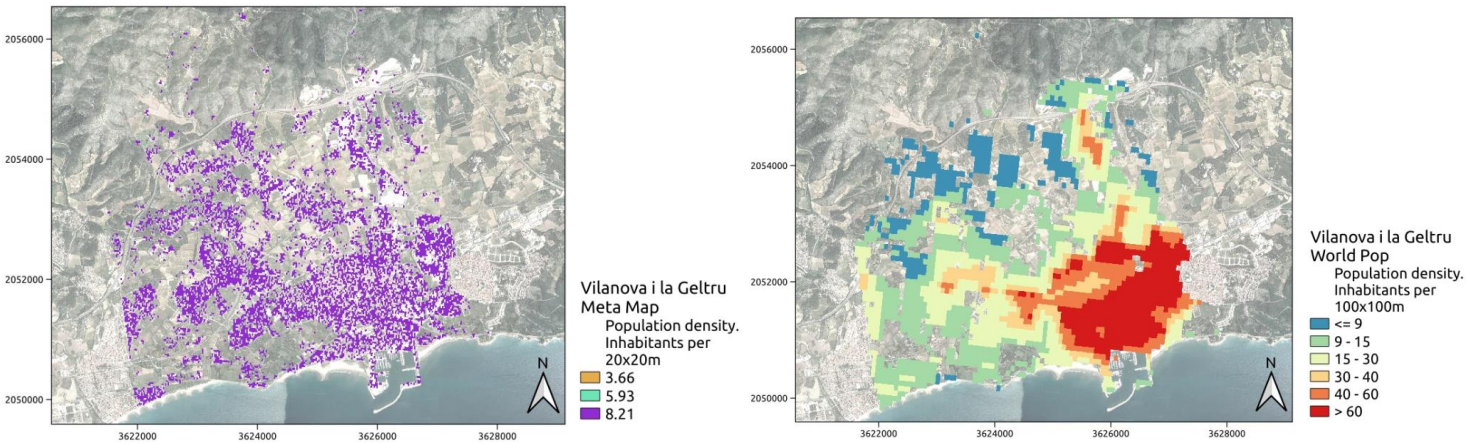

2.3.2. Methodology and outputs

The WorldPop geospatial population data were regridded to match the building exposure grip resolution and projection, thus ensuring that a consistent exposure grid is used for these two types of exposed elements. This was performed in a similar manner for the three frontrunner CCLLs, thus obtaining comparable datasets derived from a common data source.

Note that the developed population exposure maps cover the overall population distributions in the three CCLLs. Ideally, data on the geographical distributions of populations with different levels of vulnerability to natural hazards (e.g., different age groups) could be useful for a more detailed and disaggregated assessment of risk. However, such information does not exist at sub-municipality level, and therefore its inclusion in the outputs of the present task is considered irrelevant. Also, it should be highlighted that the sub-municipality population maps are associated with some degree of uncertainty, as they are derived using proxy data. Thus, while useful for the assessment of risk within a municipality, they do not represent the ground truth in an entirely accurate way, and should be used in a sensible manner.

Figure 15 to Figure 17 illustrate the regridded population exposure datasets. In Figure 15, relative to the Massa CCLL, it is possible to identify a spread distribution of the population along the coastal line, and higher population densities in the central part of the study area. Figure 16 shows how the population in Oarsoaldea tends to be concentrated along the water body, while Figure 17 shows how in the Vilanova i la Geltrú CCLL, the higher population density is distributed not only along the coastal line but also inland.

Figure 15: Massa population exposure map (CRS – EPSG:3035).

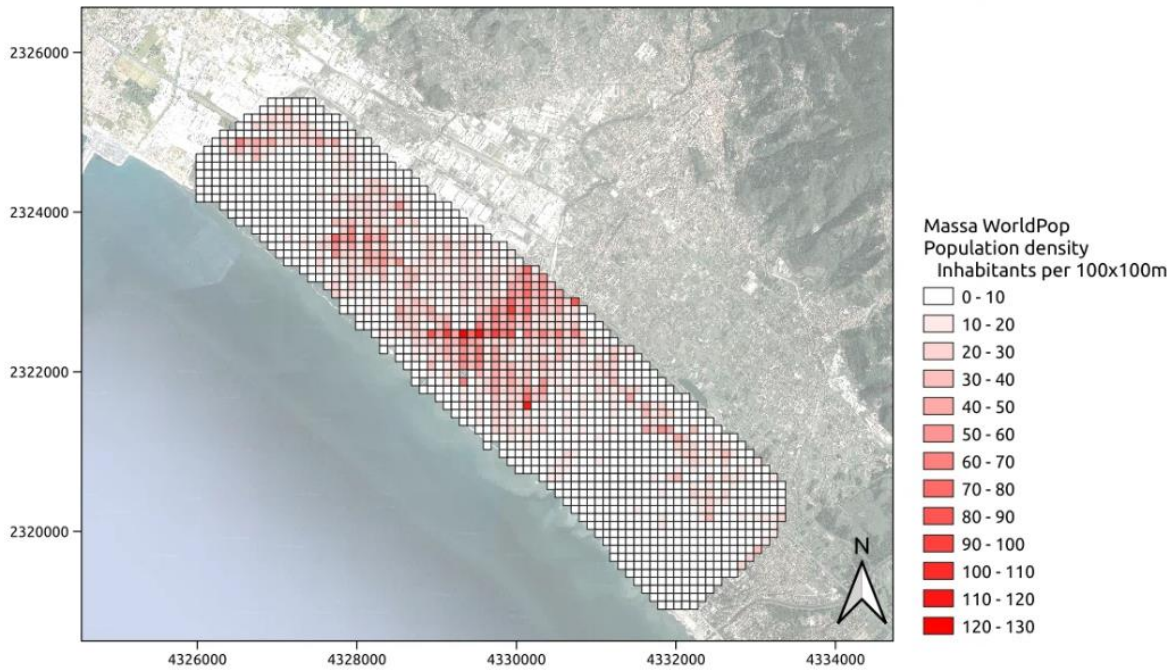

Figure 16: Oarsoaldea population exposure map (CRS – EPSG:3035).

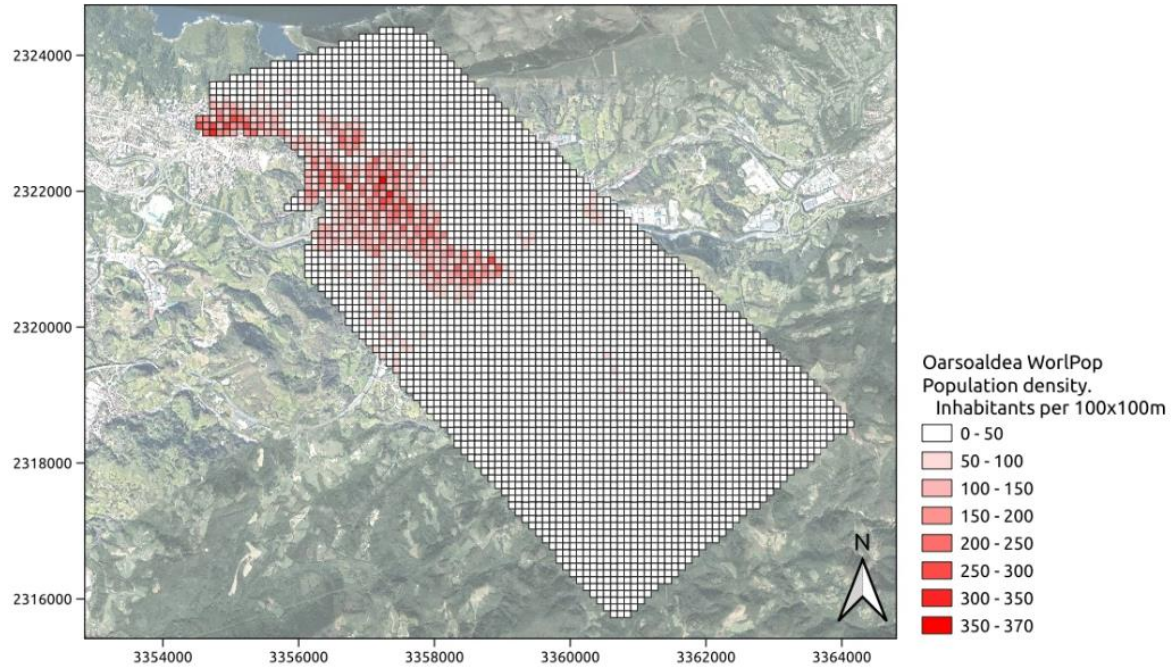

Figure 17: Vilanova i la Geltrú population exposure map (CRS – EPSG:3035).

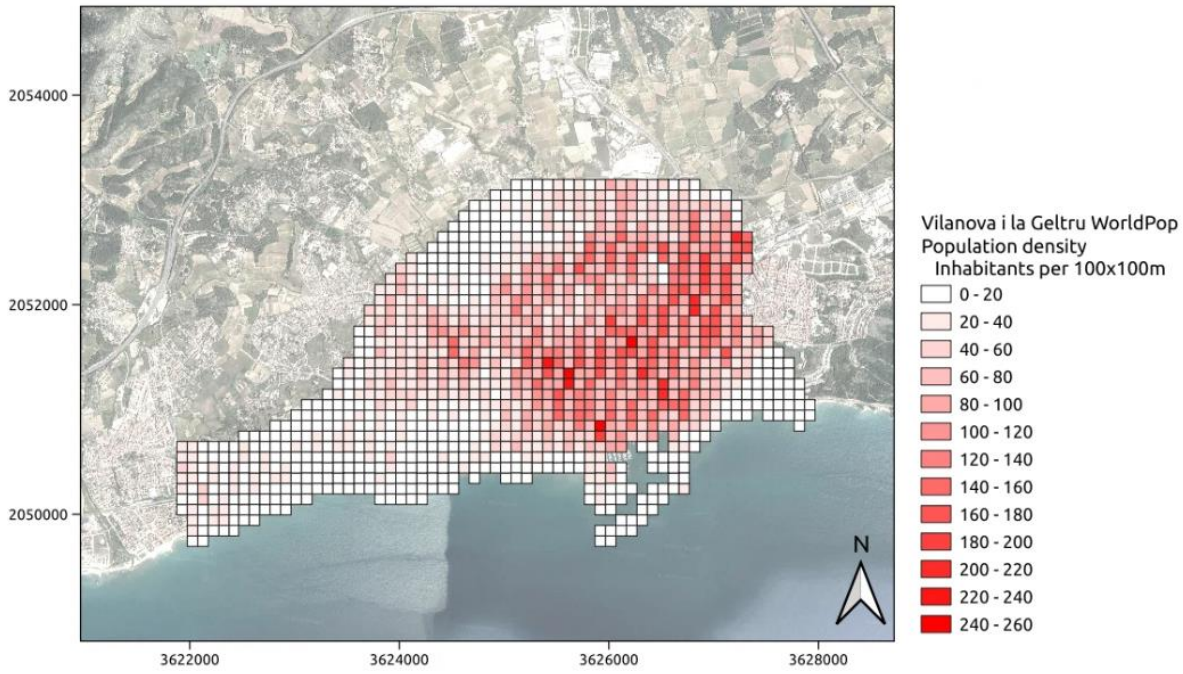

2.4. Road and railway networks

Among the different elements of the built environment, the road and railway networks are particularly relevant in the context of natural hazard risk management, including at the urban and coastal levels. In fact, the adequate functioning of transportation networks in a city is directly and indirectly related to its economy, jobs, public services, entry and exit of market and other goods, as well as emergency and relief services. Therefore, adequate risk management for these networks aligns with the United Nations Sustainable Development Goal 11, which calls for making “cities and human settlements inclusive, safe, and sustainable" (Koks, et al., 2019).

However, as reported in Peduzzi, et al., (2009), Hirabayashi, et al., (2013), and Alfieri, et al., (2017), scientific evidence is still limited on the overall impacts of natural hazards on transportation networks, both through direct damage to infrastructure and indirect impacts on users and supply chains. In fact, while many existing models for analysing disaster risk focus on damaged buildings or affected populations, transportation infrastructure is often modelled using generalized assumptions about infrastructure density rather than detailed asset mapping. In this regard, van Ginkel, et al., (2021) present one of the most recent investigations with an object-based approach, where it is estimated that the expected annual damage to the road network in Europe due to river flooding can be as high as EUR 230 million.

Regarding railway infrastructure, this transport type plays a key role in the climate-friendly transportation of freight and passengers across the European Union. According to the statistical office of the European Union (EUROSTAT), more than 415 billion passenger-kilometres were travelled, and more than 416 billion ton-kilometres were transported on national and international railway lines of the EU-28 in 2015 (Bubeck, et al., 2019). Since transport of freight and passengers by rail considerably outperforms road and air transport in terms of greenhouse gas efficiency (IPCC, 2014), it is reasonable to assume that railway infrastructure becomes increasingly important in the future. Bubeck, et al., (2019) mention that advances in the assessment of current and future risk for railway infrastructure is critical for the development of effective disaster risk management and adequate climate change adaptation planning. This is considered particularly relevant because railways constitute critical infrastructure, and losses in

public infrastructure are generally uninsured or even uninsurable in the private market. These authors examined the current and future flood risk for railway infrastructure at the scale of Europe and found that for the current scenario of 1.5 °C increasing temperature, damages could reach up to €581 million per year and with a possible increase of up to 310% under a global temperature increase scenario of 3 °C.

2.4.1. State of the art

According to the findings of van Ginkel, et al., (2021), several of the existing risk studies do not accurately represent damage to the road network for several reasons. First, these studies often use a grid-based approach to represent exposure. Infrastructure damage is typically determined by the percentage of infrastructure land-use per grid cell in land cover maps such as CORINE (Coordination of Information on the Environment) or LUISA (Land Use-based Integrated Sustainability Assessment). However, transport network infrastructure such as roads or railways are linear elements and usually occupy only a small percentage within a grid cell at continental scale (e.g., 100x100 m^2 in Europe). This can result in either an overestimation of infrastructure when it is not actually present, or an underestimation when infrastructure does exist but is not sufficient to be represented by the dominant land use type. As shown in Figure 18, there is a clear difference in the detailed representation of the transportation network between grid-based (CORINE and LUISA) and object-based approaches. Previously, the use of grid-based maps with land cover grids could be justified because exposure datasets based on continental-scale objects were incomplete. However, object-based transportation infrastructure datasets such as OpenStreetMap (OSM) are now close to being fully complete, with Barrington-Leigh and Millard-Ball (2017) claiming that most European countries have more than 95% of their roads and highways mapped in OSM.

There are other factors that have influence on the current limitations about modelling the transportation networks. According to Bubeck, et al., (2019), the following three reasons explain why damage risk modelling of railway infrastructure is still in its infancy compared to other sectors. First, public information on infrastructure elements is still considered sensitive and of limited availability. Second, there is a general absence of empirical damage data in the infrastructure sector. Third, due to their linear characteristics, railway tracks are underrepresented in land cover gridded data, which has traditionally been used for risk assessments. Such is the case, for example of the CORINE dataset, which provides spatial land cover information at a spatial resolution of 100x100 m. CORINE land use data contains a wide variety of urban infrastructure and vital elements, as shown in the left side of the Figure 18. However, CORINE overlooks the distinction of subclasses in the land cover data, causing damage modelling to lack detailed information on transportation infrastructure and adding high uncertainty to the results. Bubeck, et al., (2011) have concluded that using land-use maps, only insufficiently reflects damage modelling to linear structures. On the other hand, currently a dataset a focused in railways infrastructure called OpenRailwayMap, derived from OSM, is the most comprehensive and publicly available dataset of railway infrastructure in Europe. This dataset was used successfully also by other studies like Forzieri, et al., (2018) for assessing flood risks to critical infrastructures in Europe.

Figure 18: Comparison between the grid-based and object-based exposure datasets. Extracted from van Ginkel, et al., (2021).

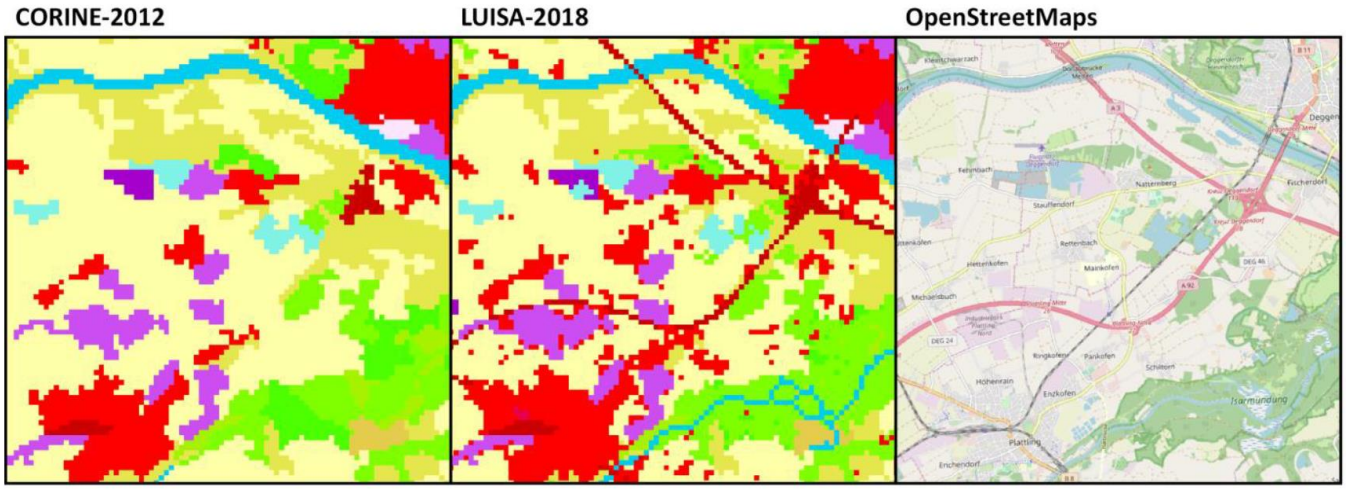

From a gridded railway track map derived from the most comprehensive European-wide dataset of OpenRailwayMap, only 2.4% of the network is coded as railway infrastructure in CORINE, despite its high resolution (Bubeck, et al., 2019). Since gridded land cover data, such as CORINE, are not sufficiently detailed to capture line-shaped infrastructure elements, the most comprehensive and publicly available dataset of railway infrastructure in Europe was derived from OpenRailwayMap or consequently OSM.

Thus, in the case of road and railway networks, object-based damage models, where the damage accounting takes place at the level of network segments, are preferable to grid-based approaches for the following reasons. First, the geometric representations have a higher resolution, allowing for more accurate intersects between the exposed roads and the hazard data. Second, object-specific attributes can be used to make more accurate damage estimates (Merz, et al., 2010). The attributes also enable the development of different damage curves for different road types (e.g., motorway or rural road), which may have very different characteristics (e.g., number of lanes, width, and quality). Third, the network properties of roads, enabling graph representations, can be maintained in an object-based approach (Gil & Steinbach, 2008).

In accordance with Koks, et al., (2019), OSM can be considered as a comprehensive and reliable global source of transportation infrastructure data, being freely accessible and downloadable with a high-resolution level of detail that successfully covers the area of Europe and many other regions in the world. OSM is distributed under the Open Database License, which is a licensing agreement designed to allow users to freely share, modify, and use a database while maintaining the same freedom for others. Around the world, there are numerous authorities, companies and other entities that provide data on road and railway networks in georeferenced form having OSM as a source of information. Among the most prominent are: Governments of the European Union countries, Great Britain, USA; large companies such as Apple and Microsoft; social networks such as Facebook, TripAvisor; GIS products such as ESRI and geojson.io, among many others.

2.4.2. Data collection

Databases of road and railway networks were provided by the three frontrunner CCLLs; however, each of the sources had different taxonomies and information elements. For this reason, in order to use a homogeneous dataset for the development of the exposure models, it was decided to consider the OSM source for both road and rail networks for

all three CCLLs. The OSM maps were obtained from the Geofabrik webpage[9] and clipped to the respective study areas.

2.4.3. Road network exposure model

2.4.3.1. Methodology

From the descriptive characteristics within the attributes of the OSM maps for the road network, those of interest are the identification number (osm_id), road class (fclass), type of direction (oneway), layer (layer), and the presence or absence of bridge (bridge) or tunnel (tunnel). Based on this information, several steps were taken to generate the road network exposure model. First, the type of road (re_class) was reclassified based on the criteria of the method proposed by van Ginkel, et al., (2021), since it is necessary to keep the same road classification in order to match in further next steps with the damage functions. Table 10 shows the reclassification key values. Second, columns were added with the number of lanes derived from the oneway value. For this, it was considered that the value "B = Both" means that the line represents two lanes of the road, while the value "F = False" means that it is only one lane. The lanes number represented by each line is important for the estimation of the unit cost of construction and repair according to the reference values. Third, by spatial cross-referencing with an additional traffic signal map (code_traff = 5201), the presence or absence (0 or 1) of accessories was determined, which according to van Ginkel, et al., (2021) can refer to electronic signalling systems and any kind of lights. This feature also makes a significant difference in determining unitary construction costs. Fourth, the column with length values in meters of the line section (length_m) was added and finally, to each of the lines the value of the average slope of the terrain in percentage (slp_per_me) derived from the MERIT Digital Elevation Model at 90 meters resolution was added. Table 11 shows an example of the contents of the exposure model dataset for roads, resulting from the process described above.

Table 10: Reclassification of the OpenStreetMap road type key values. Adapted from van Ginkel, et al., (2021).

Key values originally found in OSM	Reclassification
Motorway, motorway_link, motorway_junction	Motorway
Trunk, trunk_link	Trunk
Primary, primary_link	Primary
Secondary, secondary_link	Secondary
Tertiary, tertiary_link	Tertiary
Unclassified, residential, living_street, service, pedestrian, bus_guideway, escape, raceway, road, cycleway, construction, bus_stop, crossing, mini_roundabout, passing_place, rest_area, turning_circle, traffic_island, yes, emergency_bay	Other
Track, unsurfaced, corridor, trail, footway, path	Track
None, bridleway, steps, proposed, elevator, emergency_access_point, give_way, speed_camera, street_lamp, services, stop, traffic_signals, turning_circle, toll_gantry, stop, disused, dummy, planned, razed, abandoned (and all other unknown tags)	None

[9] https://download.geofabrik.de/europe.html

Table 11: Example of the attributes for the road network exposure models.

osm_id	fclass	re_class	oneway	layer	bridge	tunnel	lanes	code_traff	accessorie	length_m	slp_per_me
99884789	motorway_link	Motorway	F	0	F	F	2	5206	0	513.49	7.75
99884786	secondary	Secondary	B	0	F	F	2	5201	1	45.87	6.0
998471509	service	Other	B	0	F	F	1	5204	0	69.32	7.0
998471188	service	Other	B	0	F	F	1	5201	1	53.99	4.5
997126261	motorway_link	Motorway	F	0	F	F	2	5204	0	95.45	6.5

The determination of the attributes in Table 11 is also necessary to develop the taxonomy, the estimation of unit costs and the assignment of damage functions in the following steps of this methodology.

In order to validate the procedure described in the previous steps, a visual verification for lanes and accessories estimations assisted by Google Street View was conducted as shown in Figure 19. For example, the dataset element with osm_id 668159778 was verified to represent a road with two lanes and a traffic signal in Oarsoaldea (left). The central panel of Figure 19 shows the dataset element osm_id 8243009, a road in Vilanova i la Geltrú with the same previous characteristics. Lastly, the left of this figure refers to the dataset element osm_id 208784039 for Massa, with one lane and a traffic signal.

The exposure model also contains an attribute referring to the replacement costs of the road segments, which were estimated based on the methodology by van Ginkel, et al., (2021) later described in Section 3.2.2. This methodology takes into account a correcting factor that adjusts the replacements costs for each road segment based on their type (re_reclass) and number of lanes (lanes).

Figure 19: Examples of validation of road attributes using street-level imagery. Left: road in Oarsoaldea that corresponds to the value attributes of 2 lanes and with traffic signal; Centre: view of a road in Vilanova with the same attributes; Right: view of a road in Massa with one line and traffic signal.

2.4.3.2. Taxonomy

After the generation of the road network exposure model, it was necessary to name the taxonomy for each of the dataset elements. The taxonomical classes for each of the road tracks were defined as shown in Table 12, and allow straightforwardly establishing a link with the corresponding damage functions (column “Damage funct”), which are presented in more detail in Section 3.2.2. A threshold of 5% was considered to distinguish between low and high slope. The slope was included in the taxonomy because it may later be used as a proxy for the selection of vulnerability curves, which are distinguished in terms of flow velocity (i.e., specific curves for low flow velocity and high flow velocity), in case this information is not specifically provided by the hazard model. All specifications about the steps for the methodology proposed by van Ginkel, et al., (2021) are explained in the aforementioned section.

Table 12: Taxonomy codes for the roads network.

Road_type	Accessories	Lanes_number	Slope_type	Taxonomy_code	Damage funct.
Motorway	yes	1	Low slope	MOT_SOP_1L_LS	C1
Motorway	no	1	Low slope	MOT_SIM_1L_LS	C3
Motorway	yes	2	Low slope	MOT_SOP_2L_LS	C1
Motorway	no	2	Low slope	MOT_SIM_2L_LS	C3
Motorway	yes	1	High slope	MOT_SOP_1L_HS	C2
Motorway	no	1	High slope	MOT_SIM_1L_HS	C4
Motorway	yes	2	High slope	MOT_SOP_2L_HS	C2
Motorway	no	2	High slope	MOT_SIM_2L_HS	C4
Trunk	yes	1	Low slope	TRU_SOP_1L_LS	C1
Trunk	no	1	Low slope	TRU_SIM_1L_LS	C3
Trunk	yes	2	Low slope	TRU_SOP_2L_LS	C1
Trunk	no	2	Low slope	TRU_SIM_2L_LS	C3
Trunk	yes	1	High slope	TRU_SOP_1L_HS	C2
Trunk	no	1	High slope	TRU_SIM_1L_HS	C4
Trunk	yes	2	High slope	TRU_SOP_2L_HS	C2
Trunk	no	2	High slope	TRU_SIM_2L_HS	C4
Primary	yes	1	Low slope	PRI_SOP_1L_LS	C5
Primary	no	1	Low slope	PRI_SIM_1L_LS	C5
Primary	yes	2	Low slope	PRI_SOP_2L_LS	C5
Primary	no	2	Low slope	PRI_SIM_2L_LS	C5
Primary	yes	1	High slope	PRI_SOP_1L_HS	C6
Primary	no	1	High slope	PRI_SIM_1L_HS	C6
Primary	yes	2	High slope	PRI_SOP_2L_HS	C6
Primary	no	2	High slope	PRI_SIM_2L_HS	C6
Secondary	yes	1	Low slope	SEC_SOP_1L_LS	C5
Secondary	no	1	Low slope	SEC_SIM_1L_LS	C5
Secondary	yes	2	Low slope	SEC_SOP_2L_LS	C5
Secondary	no	2	Low slope	SEC_SIM_2L_LS	C5
Secondary	yes	1	High slope	SEC_SOP_1L_HS	C6
Secondary	no	1	High slope	SEC_SIM_1L_HS	C6
Secondary	yes	2	High slope	SEC_SOP_2L_HS	C6
Secondary	no	2	High slope	SEC_SIM_2L_HS	C6
Tertiary	yes	1	Low slope	TER_SOP_1L_LS	C5
Tertiary	no	1	Low slope	TER_SIM_1L_LS	C5
Tertiary	yes	2	Low slope	TER_SOP_2L_LS	C5
Tertiary	no	2	Low slope	TER_SIM_2L_LS	C5
Tertiary	yes	1	High slope	TER_SOP_1L_HS	C6
Tertiary	no	1	High slope	TER_SIM_1L_HS	C6
Tertiary	yes	2	High slope	TER_SOP_2L_HS	C6
Tertiary	no	2	High slope	TER_SIM_2L_HS	C6
Other	yes	1	Low slope	OTH_SOP_1L_LS	C5

Road_type	Accessories	Lanes_number	Slope_type	Taxonomy_code	Damage funct.
Other	no	1	Low slope	OTH_SIM_1L_LS	C5
Other	yes	2	Low slope	OTH_SOP_2L_LS	C5
Other	no	2	Low slope	OTH_SIM_2L_LS	C5
Other	yes	1	High slope	OTH_SOP_1L_HS	C6
Other	no	1	High slope	OTH_SIM_1L_HS	C6
Other	yes	2	High slope	OTH_SOP_2L_HS	C6
Other	no	2	High slope	OTH_SIM_2L_HS	C6

2.4.3.3. Outputs

The developed road network exposure models are structured in a vector data format composed of lines representing the road segments, and are saved as layers of the complete exposure dataset geopackages that are part of D6.3 of the SCORE project. In this subsection, illustrative maps of the road exposure datasets for the three CCLLs are shown by the categorization of accessories (Figure 20), slope percentage (Figure 21) and number of lanes (Figure 22). Table 13 illustrates the contents of the road exposure dataset. As explained in at the end of the Section 2.4.3.1, the method for estimating replacement costs (column named "CstE282015") are explained in Section 3.2.2.

Table 13: Illustrative table of attributes for the road exposure dataset.

osm_id	re_class	layer	bridge	tunnel	lanes	accessorie	length_m	slp_per_me	TAX_name	CstE282015
164575925	Motorway	2	F	F	2	0	485.795	0.5	MOT_SIM_2L_LS	2762959.06
721678528	Other	0	F	F	1	0	16.67	0	OTH_SIM_1L_LS	1875.37
552864134	Secondary	0	F	F	2	0	10.152	1	SEC_SIM_2L_LS	7614.01
596160099	Tertiary	0	F	F	2	1	567.121	2.5	TER_SOP_2L_LS	283560.50
227232497	Trunk	0	F	F	2	0	225.457	6	TRU_SIM_2L_HS	422731.87
38694892	Primary	-2	F	T	1	0	246.187	21	PRI_SIM_1L_HS	276960.37

Figure 20: Illustrative map of the Massa road network exposure dataset, for attribute "Accessories" (CRS – EPSG:3035).

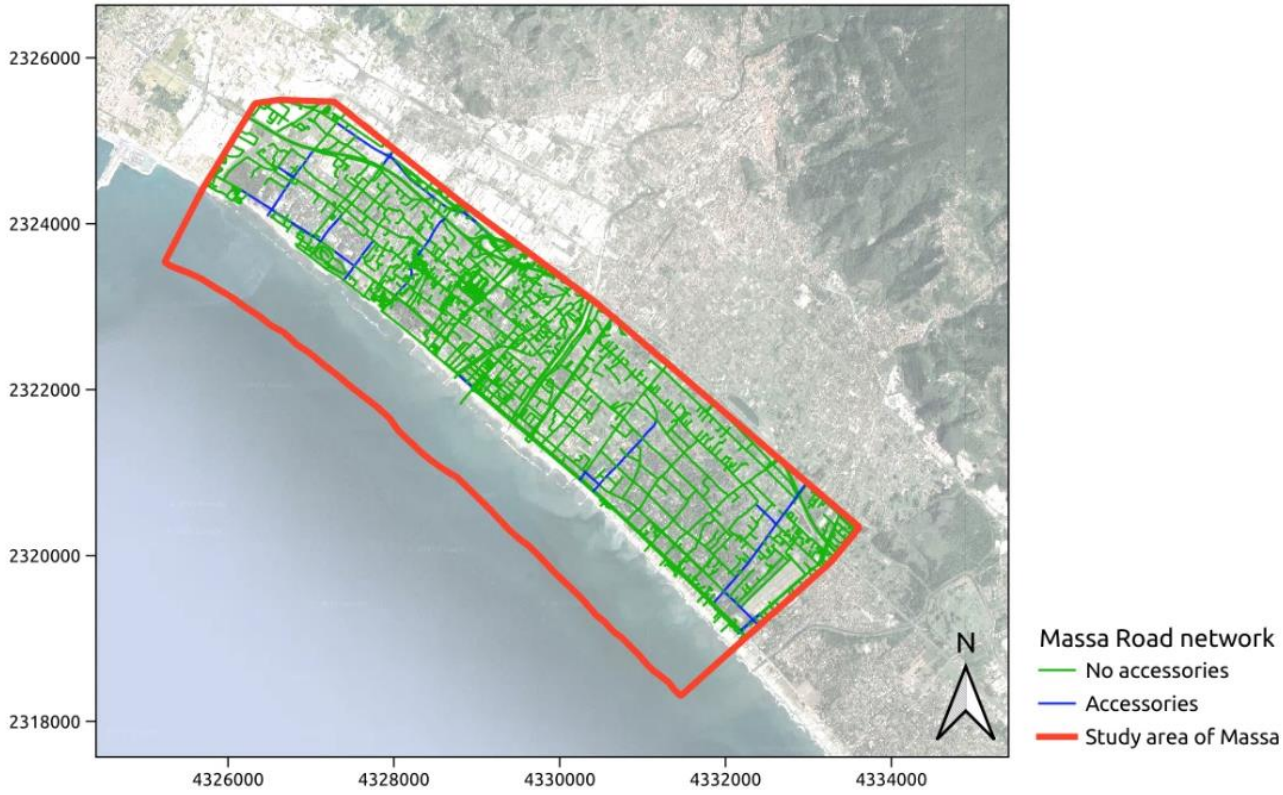

Figure 21: Illustrative map of the Oarsoaldea road network exposure dataset, for attribute "Slope percentage" (CRS – EPSG:3035).

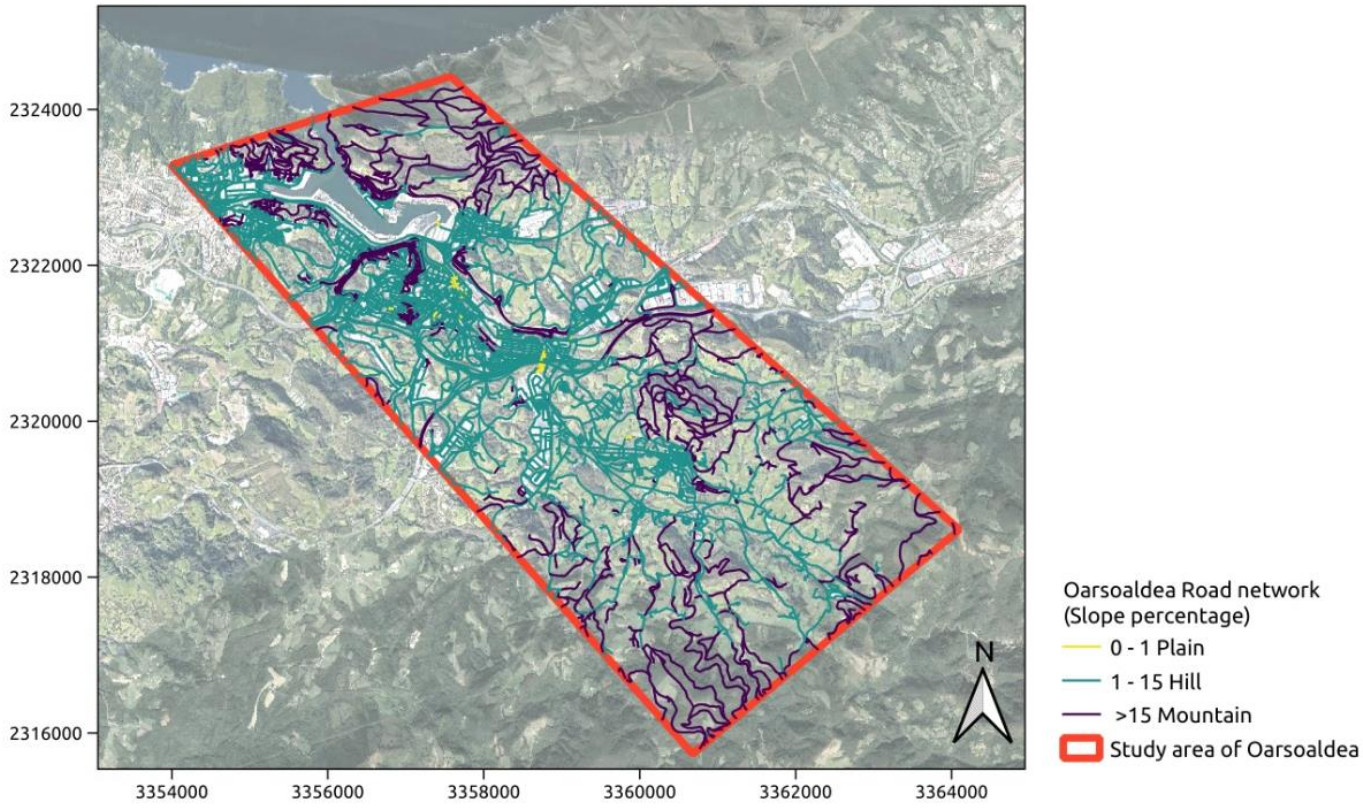

Figure 22: Illustrative map of the Vilanova i la Geltrú road network exposure dataset, for attribute "Lanes number" (CRS – EPSG:3035).

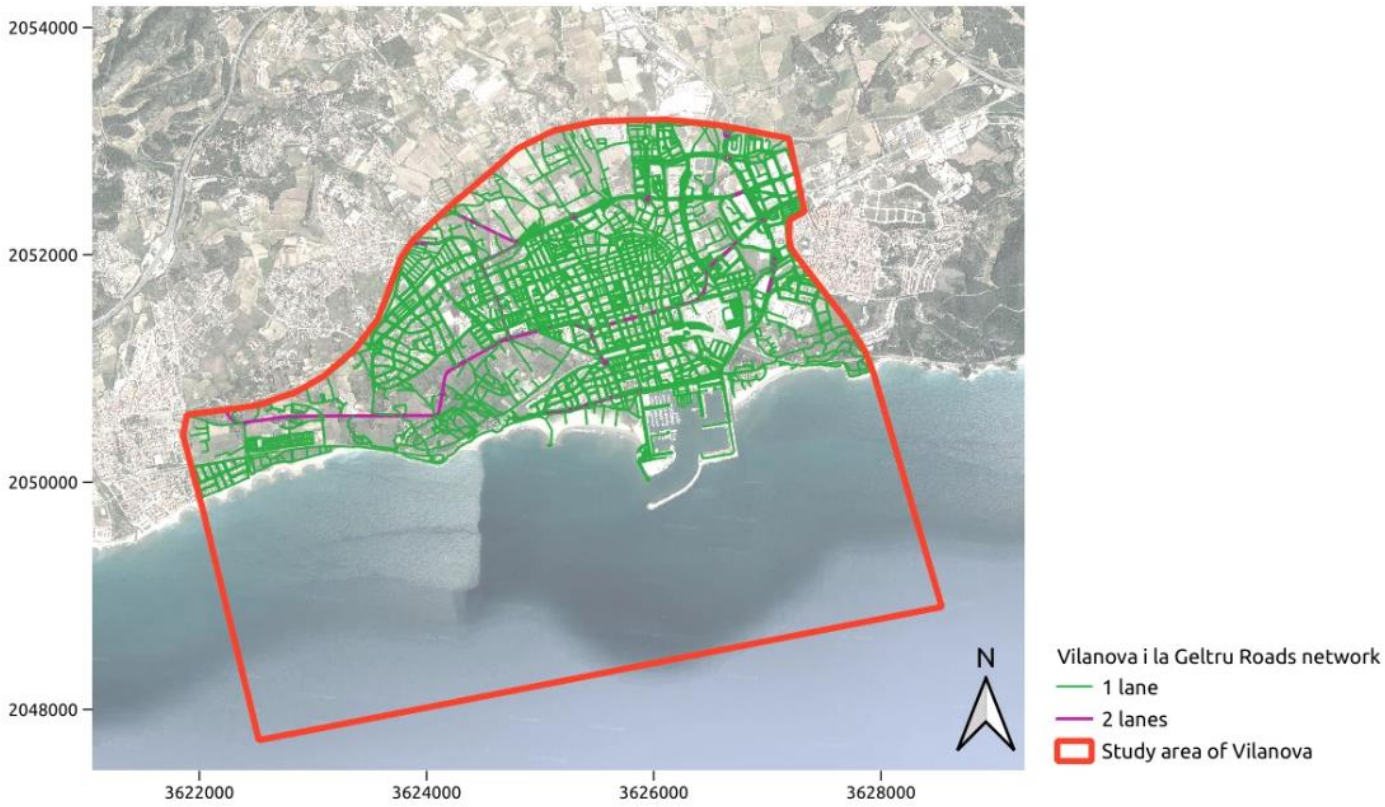

2.4.4. Railway network exposure model

2.4.4.1. Methodology

From the descriptive characteristics within the attributes of the OSM maps for the railway network, those of interest are identification number (osm_id), layer, presence or absence of tunnels (tunnel) and bridges (bridge), among others. To generate the exposure model for railways, the following steps were necessary. First, the type of railway was reclassified into underground or aboveground (re_class), since this is a crucial characteristic for flood hazards, as well as adding the value of the length in meters of the section (length_m). Second, the value of the percentage of the slope of the terrain (slp_per) was added, derived from the MERIT digital elevation model at 90 meters resolution. Third, through a visual inspection assisted by StreetView and Google Earth Pro, as shown in Figure 23, the presence of substructure or embankment (SUBstrct) and superstructure (SUPstrct) was verified, as well as the amount of railway tracks represented by the map line (Lanes). The issue of the importance of substructure and superstructure is addressed in more detail in the vulnerability section (3.2.3). Table 14 shows an example of the contents of the exposure model dataset for railways. Considering the terrain slope, it is a variable that can be related to the speed of water in a flood situation and is therefore relevant to the vulnerability section.

Figure 23: View of an Oarsoaldea's railway track by Google Earth Pro (left) and view of a Vilanova's railway track by Google Street View (right).

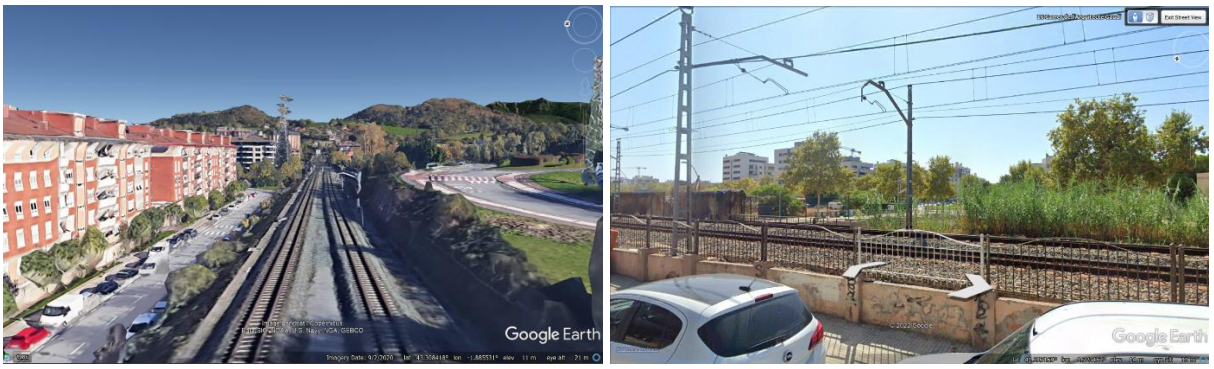

Table 14: Attributes for the railway exposure model

osm_id	re_class	layer	bridge	tunnel	slp_per	SUBstrct	SUPstrct	Lanes	length_m
120719846	Aboveground	1	T	F	4.07	1	1	1	159.73
120719847	Aboveground	1	F	F	3.49	1	0	1	37.70
146392616	Aboveground	0	F	F	7.57	0	1	1	238.14
146392618	Aboveground	0	F	F	1.74	1	1	1	69.98
146392619	Aboveground	-1	F	F	3.49	1	1	1	37.34
146392620	Aboveground	-2	T	F	2.61	0	0	1	51.32

A characteristic of the three CCLLs in this study is that none of them have underground railway infrastructure. In their entirety, all railways are of the surface type, even in the case of tunnels. The presence of tunnels and bridges contains the variables TF (True, False), while the column "layer" refers to the level where the line is located on the map with values ranging from -5 to 5 according to the official OSM description. For example, 0 corresponds to a section at ground level, while 1 (or more) means that the line passes one level (or more) above the ground and other sections as in the case of bridges. Analogously, negative values represent underpasses (not considered as underground). The meaning of "layer" applies in the same way to the road exposure model.

The substructure includes the embankment to support the rails and sleepers, while the superstructure comprises all the accessories such as spans, poles and cables, arches, etc., which are located on top of the rails. The identification of these elements is equally of significant importance for the determination of vulnerability and damage cost in the following steps of this report. Finally, the number of railway tracks that each line in the dataset represents is determining for the relationship with reference values on construction or repair costs.

2.4.4.2. Taxonomy

Following with the railway exposure dataset, a taxonomy was generated. The taxonomy is composed of 4 possible combinations of railway track characteristics, varying according to the presence or absence of the substructure and superstructure, as shown in Table 15. The taxonomical codes are used in conjunction with the hazard maps of water height (data provided in D3.7) during the risk modelling to determine the damage cost in absolute terms, as will be explained in Section 3.2.3.

Table 15: Taxonomy codes for the railways

Railway type	Substructure	Superstructure	Taxonomy code
Railway	yes	yes	RAIL_SUB_SUP
Railway	yes	no	RAIL_SUB_NOSUP
Railway	no	yes	RAIL_NOSUB_SUP
Railway	no	no	RAIL_NOSUB_NOSUP

2.4.4.3. Outputs

As a result, railway exposure models were obtained for the Oarsoaldea and Vilanova i la Geltrú CCLLs. For the case of Massa CCLL, the railway network tracks is located outside the respective study area. Table 16 shows the example of the content for the table of attributes for each railway track in the exposure dataset. In the Figure 24 is shown an illustrative map for the city of Oarsoaldea with the distribution of the attribute of terrain slope percentage, while Figure 25 is shown a, illustrative map for the city of Vilanova i la Geltrú for the presence or absence of substructure and superstructure in the railway tracks of the exposure dataset.

Table 16: Illustrative table of attributes for the railway exposure dataset.

osm_id	re_class	layer	bridge	tunnel	slp_per	SUBstrct	SUPstrct	Lanes	length_m	Tax_code
178992510	Aboveground	-1	F	T	0.90	96	1	1	1	RAIL_SUB_SUP
992312007	Aboveground	0	F	F	0.90	189	1	1	1	RAIL_SUB_SUP
91790126	Aboveground	1	T	F	0.90	10	1	1	1	RAIL_SUB_SUP
265572329	Aboveground	0	F	F	0.91	420	1	1	1	RAIL_SUB_SUP
214787693	Aboveground	0	F	F	0.93	64	0	0	1	RAIL_NOSUB_NOSUP
492380271	Aboveground	0	F	F	0.95	196	0	1	1	RAIL_NOSUB_SUP
492380272	Aboveground	0	F	F	1.03	175	0	1	1	RAIL_NOSUB_SUP

Figure 24: Illustrative maps of the Oarsoaldea railway network exposure model, with segments classified according to the slope of the terrain where they are located (CRS – EPSG:3035).

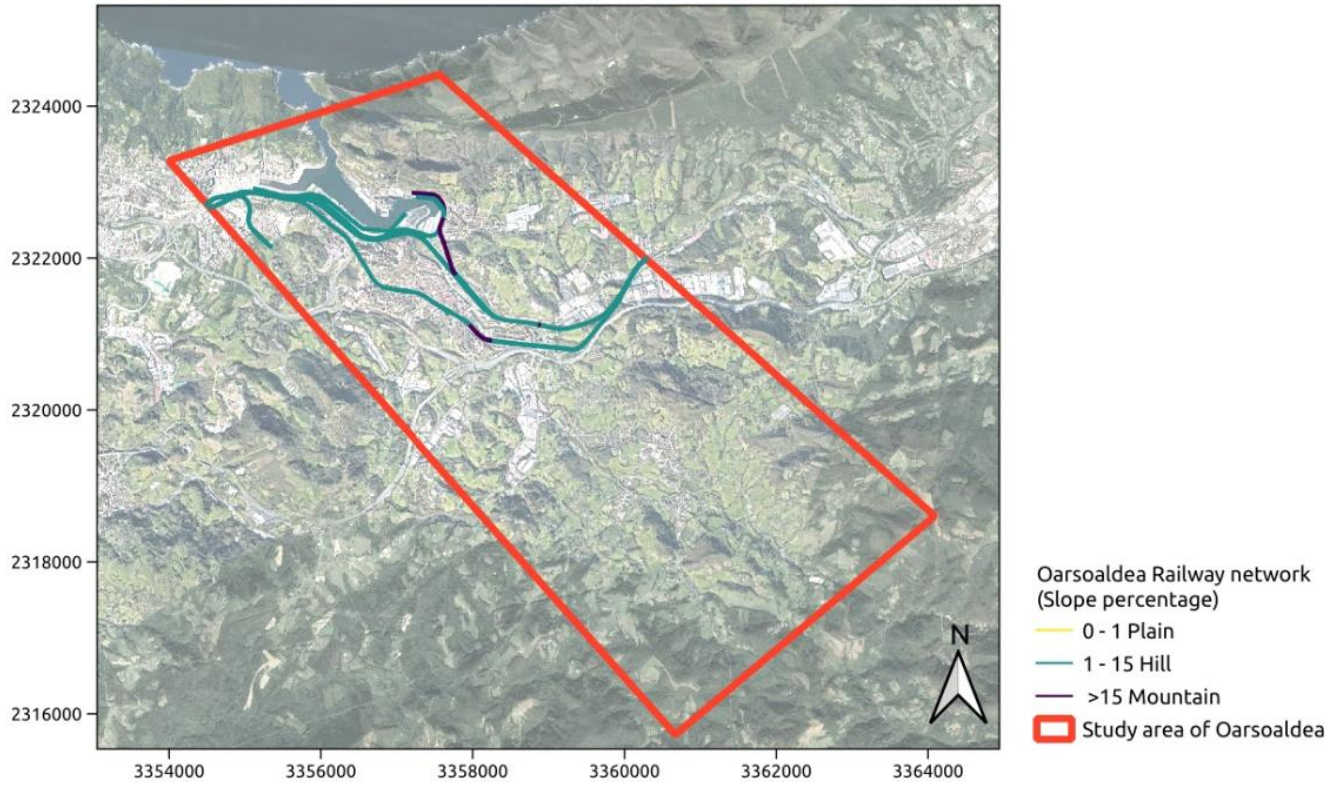

Figure 25: Illustrative map of the Vilanova i la Geltrú railway network exposure model, with segments classified according to the presence of substructure and superstructure (CRS – EPSG:3035).

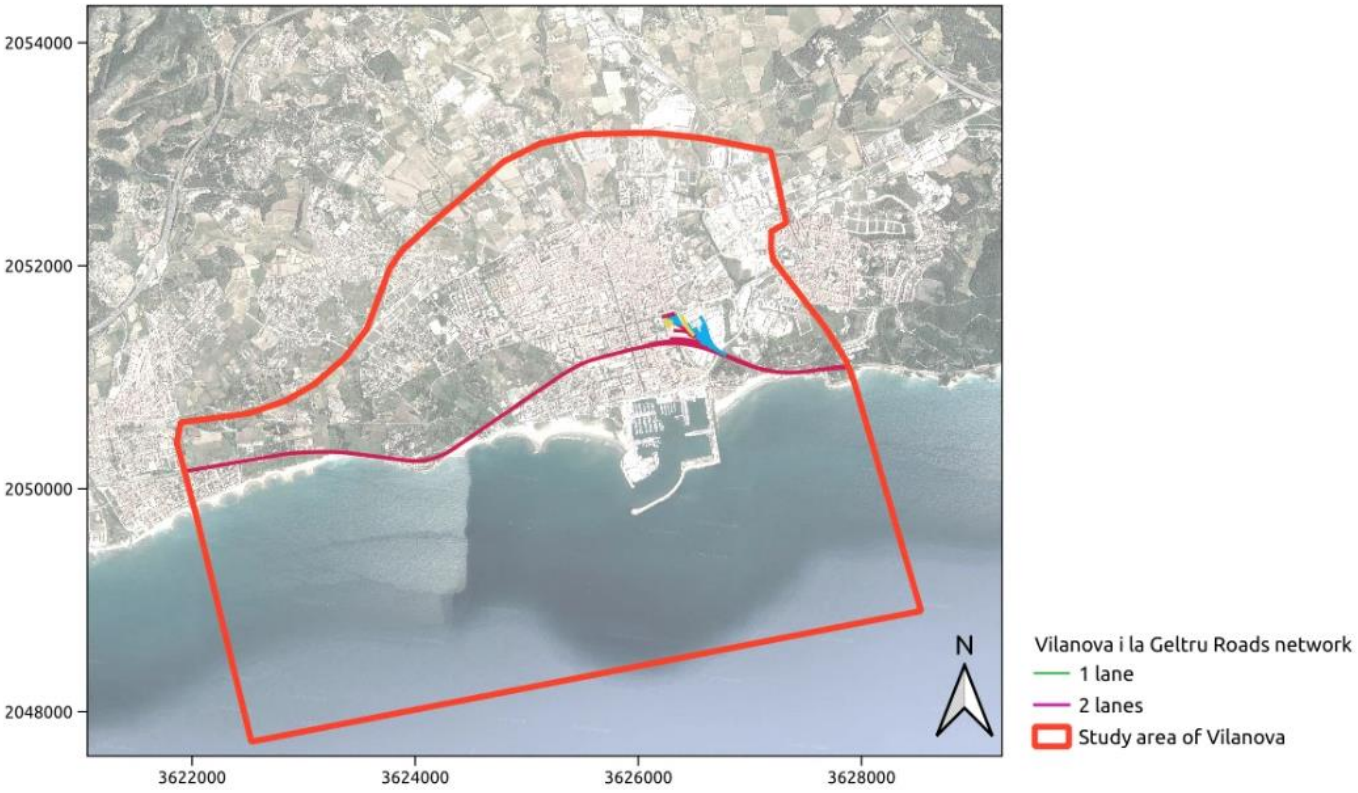

3. VULNERABILITY

The vulnerability component of catastrophe risk models comprises the models that can be used to establish mathematical relationships between hazard intensity and resulting damage and losses for different types of assets. This section provides a brief state of the art relative to vulnerability modelling of the asset types considered in this project, i.e., buildings and transportation networks, and presents the methodology adopted for each of them. For population, no vulnerability functions are required as risk will be expressed in terms of number of affected persons.

3.1. Buildings vulnerability

Flood vulnerability models for buildings are generally classified according to the underlying modelling framework. In this regard, two main approaches exist: empirical and synthetic. Empirical models are developed using data from past flood events to link hazard and vulnerability variables. This requires knowledge of the economic losses that occurred at a sufficiently large number of buildings during a previous flood event, and information about the hazard intensity at the same locations, in order to construct a predictive model. However, the necessary post-event flood loss data are seldom collected in a systematic way and tend to be heterogeneous and/or have low quality. Moreover, existing data are often not available for research purposes (Merz, et al., 2010). Another central issue with empirical flood vulnerability models is that they have been shown to have limited predictive ability when a spatial transfer is involved, i.e., when a model developed based on data for a given location is used to predict flood losses at another location. However, in practical applications it is often the case that no models are available to estimate flood losses at specific locations of interest, as is the case, to the best of our knowledge, for the three frontrunner CCLLs. In this type of situation, most empirical flood loss models are generally considered unreliable (Cammerer, et al., 2013).

On the other hand, synthetic flood vulnerability models are developed through an expert-based approach based on knowledge and assumptions about flood damage mechanisms. Typically, this is achieved by performing what-if analyses, whereby hypothetical flood scenarios are simulated and the corresponding damage and losses to different types of buildings and/or building components are quantified. Synthetic models can be particularly useful when flood loss data and/or other models are scarce or non-existent for a given application case. In fact, because this modelling approach is based mainly on engineering knowledge and expertise, it is less dependent on observational data for model development. However, synthetic models are not as common in the literature as empirical models.

In order to establish flood vulnerability functions to be used in the context of the present WP, an extensive literature review was carried out. This covered not only recent review articles on the subject of flood vulnerability, but also a screening of selected research articles both on the development of individual empirical and synthetic models and on model comparison and benchmarking research efforts (Amadio, et al., 2019; Galasso, et al., 2021; Gerl, et al., 2016; Molinari, et al., 2020). Ultimately, this provided a robust basis for selecting a set of models that are considered appropriate for application in the present WP. Accordingly, the adopted methodologies are presented in the following subsection.

As a final remark, it is important to highlight that regardless of the model(s) that is(are) adopted in any application case, vulnerability modelling remains a field where high levels of uncertainty are to some extent unavoidable (Figueiredo, et al., 2018; Schröter, et al., 2014), and this should be taken into consideration when performing flood risk assessments.

3.1.1. Methodology and outputs

In order to define a vulnerability modelling approach for this task, various criteria were considered. First, the approach should be consistent and applicable to the three CCLLs. Second, the underlying models should be

adequately documented and, more importantly, openly available, not only for the sake of result reproducibility but also to allow for possible future adjustments if they are found to be necessary. Third, the models and associated publications should have proven scientific merit and recognition, expressed by metrics such as the number of scientific citations and application in loss and risk assessment studies. Lastly, the models should be able to express damage in relative terms, i.e., as a fraction of building replacement costs, such that they can be used together with the developed exposure models, where value is expressed in that manner. Taking into account the taxonomy defined and presented in the previous section, two main models were adopted, INSYDE and JRC, which are presented in the respective subsections below. Note that these models, similarly to most models available in the literature, generally refer to fluvial flooding. In principle, modelling outputs can also be applicable also to coastal floods, but may require adjustments to reflect specific properties of coast floods, such as the presence of saltwater or higher flow velocities. This issue will be addressed in subsequent WP6 activities related with quantitative risk assessment if deemed necessary.

3.1.1.1. INSYDE

The INSYDE model (Dottori, et al., 2016) is a synthetic flood vulnerability model developed for residential buildings. The model is available as open source software[10]. It has been applied for the assessment of flood losses in several studies and different contexts and scales, and has been shown to be able to generally provide accurate flood loss estimates (e.g., Amadio, et al., 2019; Molinari, et al., 2020). INSYDE is a component-based vulnerability model, meaning that building losses are estimated as the sum of individual losses calculated for the different types of flood damage that are assumed to occur in different building types as a result of flood actions. The different loss components refer to clean-up and removal costs, structural damage, non-structural damage, damage to finishing elements, damage to windows and doors, and damage to building systems. Each of these components is further divided into subcomponents that refer to the specific repair and/or replacement of works for the different building elements. The list of components and subcomponents is shown in Table 17. For each subcomponent, INSYDE contains a set of mathematical functions that describe the corresponding physical damage mechanisms and associated cost. These functions, which account for the properties of the hazard and characteristics of the building, were defined based on expert engineering knowledge, technical documentation and scientific literature. For details about the specific damage and loss estimation method for each building subcomponent, and more information on the general methodology, the reader is referred to the original research article (Dottori, et al., 2016) and to its supplementary material.

[10] https://github.com/ruipcfig/insyde

Table 17: Damage components and subcomponents considered in the INSYDE model. The codes of the subcomponents are taken from the original publication.

Damage components	Damage subcomponents
Clean-up	C1 - Pumping
	C2 - Waste disposal
	C3 - Cleaning
	C4 - Dehumidification
Removal	R1 - Screed
	R2 - Pavement
	R3 - Baseboard
	R4 - Partition walls
	R5 - Plasterboard
	R6 - External plaster
	R7 - Internal plaster
	R8 - Doors
	R9 - Windows
	R10 - Boiler
Non-structural	N1 - Partitions replacement
	N2 - Screed replacement
	N3 - Plasterboard replacement
Structural	S1 - Soil consolidation
	S2 - Local repair
	S3 - Pillar repair
Finishing	F1 - External plaster replacement
	F2 - Internal plaster replacement
	F3 - External painting
	F4 - Internal painting
	F5 - Pavement replacement
	F6 - Baseboard replacement
Doors and windows	W1 - Doors replacement
	W2 - Windows replacement
Building systems	P1 - Boiler replacement
	P2 - Radiator painting
	P3 - Underfloor heating replacement
	P4 - Electrical system replacement
	P5 - Plumbing system replacement

The INSYDE model is able to provide loss figures both in absolute monetary values as well as in relative terms; here, interest is on the latter, as explained in above. It should also be noted that although INSYDE can be employed to estimate losses on a building-by-building basis, taking into account detailed information of individual building characteristics, it is equally suitable for application at larger scales, for sets of building sharing similar characteristics. In order to achieve this aim, the INSYDE model is used to derive vulnerability functions that can be associated to the taxonomical classes in the exposure database, particularly those referring to residential/mixed use buildings or buildings types that can be assumed to have similar typologies. In this case, vulnerability functions were developed for buildings of different material classes and with/without basement. Note that INSYDE is able to take several other building-related data as input variables (albeit generally less informative for the estimation of relative flood losses than building material and presence of basement), but in larger-scale applications where such data are not available, default values representing the most typical cases can be assumed.

Also note that INSYDE is a multivariate model that is able to estimate losses as a function of several hazard variables such as water depth, flow velocity or flood duration. Nevertheless, water depth is generally the most informative flood intensity measure for explaining flood losses and is also the most widely used in flood hazard models. Therefore,

and also for coherence with the JRC-based vulnerability functions described in the following subsection, the vulnerability functions derived with INSYDE for this task are depth-damage functions, i.e., functions that express losses in relative terms as a function of water depth. For other hazard input data, INSYDE's default values (which reflect the most typical flood conditions) were adopted.

Based on this, depth-damage functions were derived by performing a simulated step-wise inundation for four building typologies (reinforced concrete and masonry buildings with and without basement) and estimating the corresponding relative damages. The functions are shown in Figure 26 and provided in tabular form as part of D6.3. The correspondence between the functions and the exposure model taxonomical classes is presented in Table 18. Here, no reference is made to the height class because the functions are designed to provide damage estimates for the buildings' ground floor (and basement, when it is assumed to exist) regardless of the number of storeys. Thus, to estimate losses, they are meant to be used together with the exposure dataset containing the replacement costs considered as potentially exposed to flooding.

Figure 26: Depth-damage functions for buildings derived using the INSYDE flood vulnerability model.

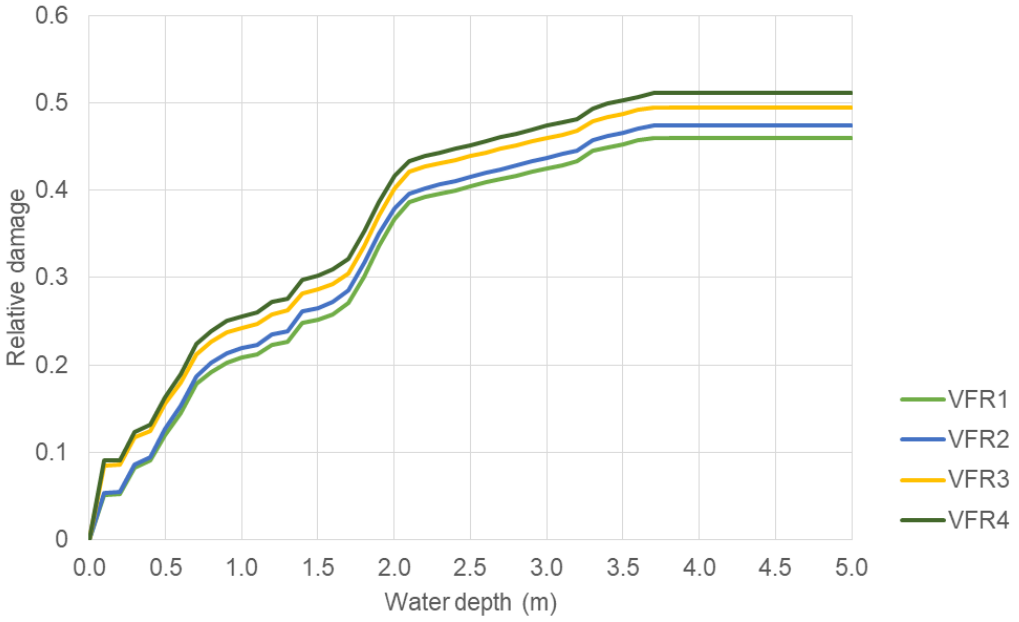

Table 18: Applicability of the vulnerability functions developed using the INSYDE model to the exposure model taxonomical classes.

Vulnerability function code	Taxonomical classes
VFR1	RESMIX_RC RESMIX_OTH PUBLIC_RC
VFR2	RESMIX_MSN PUBLIC_MSN
VFR3	RESMIX_RC_B RESMIX_OTH_B PUBLIC_RC_B
VFR4	RESMIX_MSN_B PUBLIC_MSN_B

3.1.1.2. JRC

Flood vulnerability functions are much more common for residential buildings than for other building types. Accordingly, relatively few models for estimating flood losses to industrial and/or commercial are available in the literature. Therefore, in order to establish functions for the assessment of flood losses to these building typologies, the methodology and vulnerability functions developed by JRC for application worldwide were adopted (Huizinga, et al., 2017). Even if these functions refer to generic building typologies, they have the advantage of being readily available as well as well-known and widely applicable in the flood loss modelling field. The JRC approach comprises three main components: 1) vulnerability depth-damage functions that express damage in relative terms for various types of buildings and infrastructure; 2) guidelines on how to adjust the provided functions to specific application cases; and 3) reconstruction costs that can be combined with the depth-damage functions to estimate absolute loss figures. For the vulnerability modelling part of the present task, interest is on the first two points; point 3 was taken into account in the definition of consistent building replacement costs, as explain in Section 2.2.3.2.

The JRC database contains baseline functions, where relative damage always ranges from 0 to 1, is provided for specific water depths. The functions are meant to then be scaled by a factor that reflects the parts of the buildings considered undamageable. The starting point for the definition of the vulnerability functions for buildings of the INDCOM taxonomical class were the two JRC functions relative to industrial and commercial buildings in Europe. First, a new function was defined the mean values of these two functions (which are very similar), and a linear interpolation was used to obtain water depths in smaller steps, for coherence with the functions produced using INSYDE. It was then necessary to define the undamageable part factor. For residential, industrial and commercial buildings made of generally resistant materials, as is generally the case in the target CCLLs, the JRC methodology provides a reference value of 0.60 for the maximum possible relative damage. Based on this, a finer differentiation of the buildings' vulnerability based on their materials was not performed. For consistency with the functions developed using the INSYDE model, and based on expert judgement, the maximum relative damage was defined as the mean of the maximum relative damages previously obtained (approximately 0.50). For the definition of the vulnerability for buildings with basement, the relative differences in damage between buildings with and without basement from the INSYDE model for each water depth step were applied. The developed functions are shown in Figure 27 and provided in tabular form as part of D6.3. The correspondence between the functions and the exposure model taxonomical classes is presented in Table 19.

Figure 27: Depth-damage functions for buildings derived using the JRC flood vulnerability model.

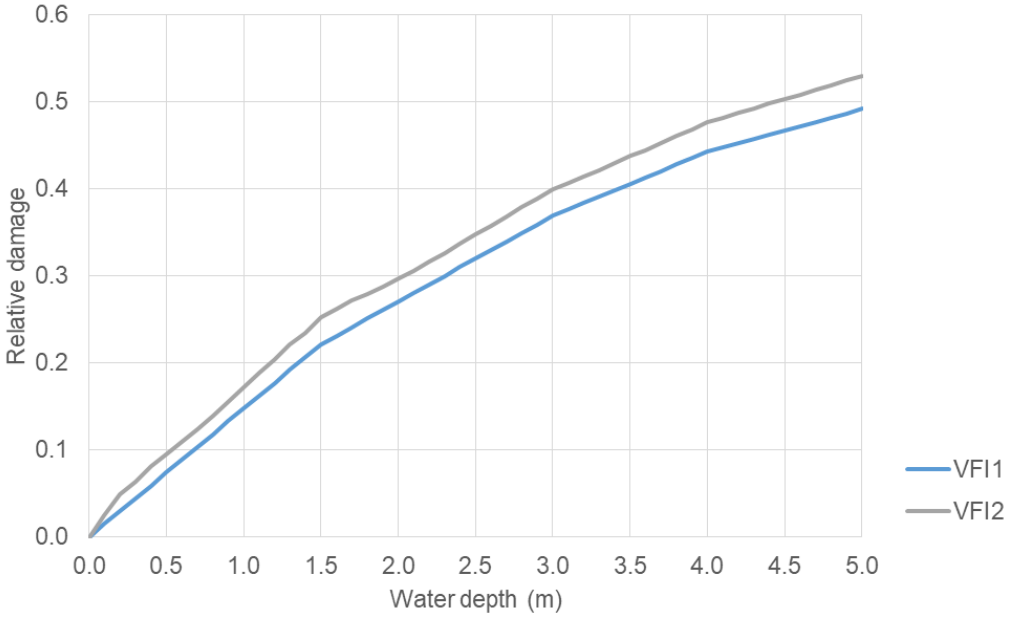

Table 19: Applicability of the vulnerability functions developed using the JRC database to the exposure model taxonomical classes.

Vulnerability function code	Taxonomical classes
VFI1	INDCOM_RC INDCOM_MSN INDCOM_STL PRTBLD_RC PRTBLD_MSN PRTBLD_STL
VFI2	INDCOM_RC_B INDCOM_MSN_B INDCOM_STL_B PRTBLD_RC_B PRTBLD_MSN_B PRTBLD_STL_B

3.2. Road and railway network vulnerability

Recently, the modelling of critical infrastructure of transport networks (roads and railways) and their behaviour during climate-related extreme events has gained attention (Habermann & Hedel, 2018). The vulnerability assessment of complex systems such as transportation infrastructure requires the use of an integrated framework, which should include analytical methods to investigate the problem from a range of perspectives (Papilloud & Keiler, 2021). Naturally, the cornerstone of such analyses is the quantitative assessment of the physical vulnerability of the components of these networks.

3.2.1. State of the art

In the work of van Ginkel, et al., (2021), it is noted that almost all transportation network flood risk studies across Europe rely on the set of damage curves proposed by Huizinga, et al., (2017), which are available in a standardized form for all continents. These were developed for coarse grid-based assessments of transport infrastructure and are considered to lack sufficient detail for the accurate damage assessment of these networks. However, the fact is that

flood vulnerability functions for transportation networks are not common in the literature. Among them, flood vulnerability curves for railways are particularly scarce and, despite the potential damage they can suffer from a flood, have received less attention compared to the flood vulnerability of roads. As a result, the same vulnerability curve used for roads is often also assigned to railways, as in the Dutch Standard Method (Kok, et al., 2004) and its updated version, the Standard Damage and Fatality assessment model 2015 named SSM2015 (de Bruijn, et al., 2015). Kellermann, et al., (2015) used the generic "infrastructure" curve from the Damage Scanner model (Klijn, et al., 2007) for railways in Austria. Wang, et al., (2021) adjusted the SSM2015 model to adapt it for countries other than the Netherlands. Habermann & Hedel (2018) also concluded that damage functions for roads and railways are often united or mentioned as one and the same. Among the authors who explicitly mention railways in their damage functions are Deckers, et al., (2010), Kok, et al., (2004), Vanneuville, et al., (2003) and Verwaest, et al., (2008). Examples of damage functions for flood hazard for two of these sources are shown in Figure 28.

Figure 28: Flood damage functions for roads and railways in relation to water depth. The sources are Kok, et al., (2004) at left and Vanneuville, et al., (2003) at right. Extracted from Habermann & Hedel (2018).

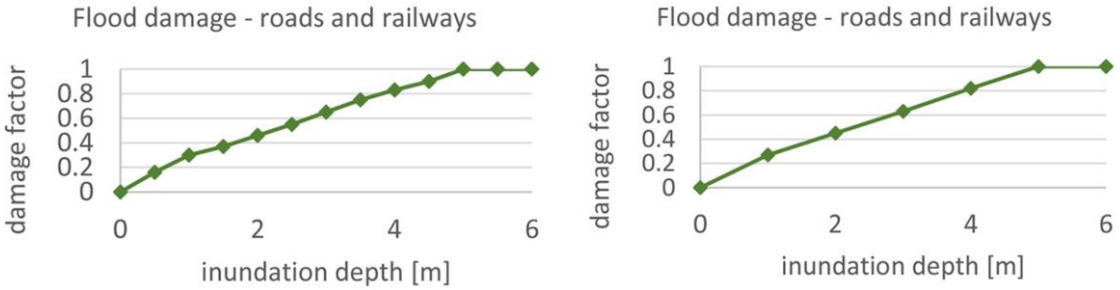

The authors de Brujin, et al., (2015) indicate that little is known about the flood vulnerability of railways. The same authors proposed the depth-damage function for roads and railways shown in the Figure 29. These infrastructures are not considered particularly vulnerable for low water depths (<25 cm), while for larger water depths the electric infrastructure is hit, hence increasing rapidly the level of damage; finally, the function becomes less steep after a point where additional water is not expected to significantly increase the damage.

Figure 29: Flood damage function proposed by de Brujin, et al., (2015) for roads and railways.

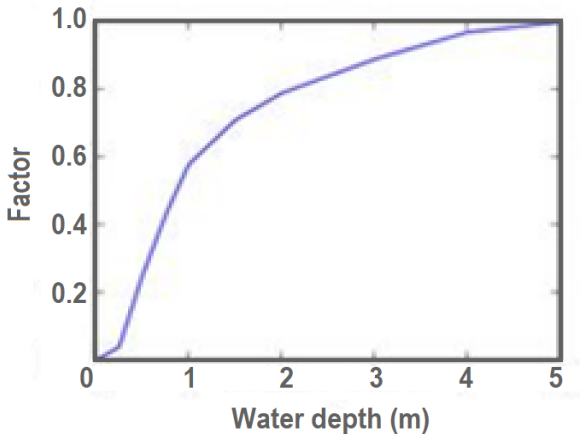

Large-scale models for transportation networks typically work with functions relating damage to water depth only (Alfieri, et al., 2016a; de Moel, et al., 2015; Winsemius, et al., 2013). Flow velocity, however, can in certain situations also be informative for explaining flood damage to roads (Merz, et al., 2010; Thieken, et al., 2009). In fact, while under low-flow velocities (<0.2 ms^{-1}) there is hardly any structural damage to pavements, under high-flow velocities (>2.0 ms^{-1}) structural damage is more likely to occur (Kreibich, et al., 2009).

In this context, for road networks, van Ginkel, et al., (2021) developed a new set of six depth-damage functions differentiating between three dimensions: road type, road accessories, and flow velocity. These damage functions cover various aspects of the direct tangible costs, including clean-up costs, resurfacing of top and deeper asphalt layers, repairs of road embankments, and where applicable also the repair of electronic signalling and lighting. It does not include structural damage to bridges and tunnels or indirect costs.

On the side of railway damage modelling, Kellermann, et al., (2015) developed a model for flood damage estimation for railway infrastructure called RAIL (Railway Infrastructure Loss). This model was derived from empirical flood damage data during and after the 2006 Morava River flood in Austria. RAIL is capable of estimating the expected structural damage to the cross-section of railways using the water depth as a reference, as well as estimating the resulting repair costs. During its development, RAIL was compared with two other damage estimation models that are based on depth-damage curves, RAM (Rhine Atlas damage model) and DSM (Damage Scanner model) and was shown to be more accurate.

3.2.2. Methodology for the road network vulnerability

In the present task, the flood vulnerability model recently presented by van Ginkel, et al., (2021) was selected to represent flood vulnerability of road networks. It comprises various innovative aspects in relation to other models in the literature, namely being specifically designed for object-based assessments and providing various functions for roads with different characteristics, distinguishing them according to certain key features that are meaningful for more accurately estimating flood losses. The model is based on European empirical data and has been successfully applied for the flood risk assessment of roads at the continental level.

The model provides six vulnerability functions that differentiate among road types, road accessories and flow velocity, as shown in Figure 30. Regarding road types, motorways and trunk roads are distinguished from other roads due to higher maintenance standards, reflected in higher reconstruction costs. Also, these are often built on top of embankments (substructure) so that relatively little damage occurs when the top of the road embankment is not yet reached, represented by a concave section in the beginning of curve C1– C4 in the Figure 31. The other road categories (primary, secondary, tertiary, and other roads) are usually not built on top of embankments, and their curves (C5 and C6) therefore do not present the same concave shape at lower water depth (Figure 31). Next, motorways and trunk roads with sophisticated accessories such as electronic traffic management systems, lighting, and noise barriers (C1 and C2) are differentiated from simple roads without these accessories (C3 and C4). This represents the large spread in construction costs in Figure 31, between simple and sophisticated motorways and trunk roads and the corresponding extra damage that may occur to the electronic signalling and lighting of sophisticated roads, even under low-flow conditions. Finally, low-flow conditions (C1, C3, and C5) are distinguished from high-flow conditions (C2, C4, and C6).

Figure 30: Dimensions used for differentiating the damage curves (C1–C6) in van Ginkel, et al., (2021).

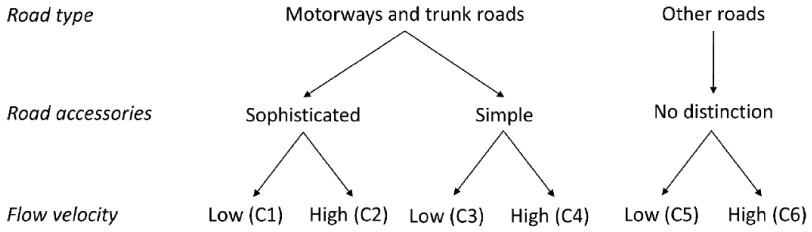

Figure 31: Damage curves (C1 to C6) for illustrative values of road construction costs, in euros per kilometer. Extracted from van Ginkel, et al., (2021).

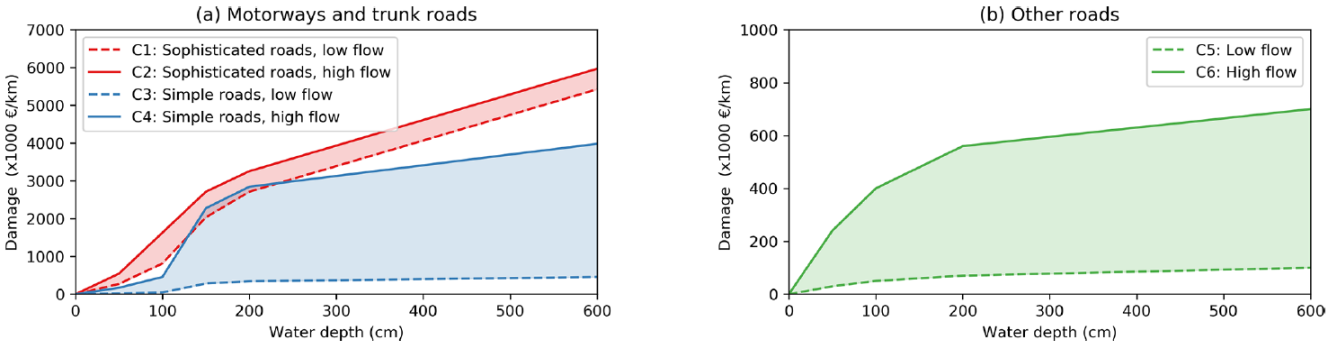

To use the proposed method, the damage curves are expressed as fraction of the road construction costs (as explained following in step 3) and they are to be multiplied with the construction cost established for road type in Table 20. The protocol established to construct the object-specific depth-damage curves by van Ginkel, et al., (2021) consists in 4 steps as follows:

Step 1: determine the minimum and maximum construction cost per road type

It is important to clarify that the data in the Table 20 are the corrected construction costs to represent the year 2015 for the former EU-28 (European Union with 28-member states), and expressed in average price levels per kilometre. Later in the method, an adjustment will be made for both the current year and the specific country.

Then, using the taxonomy codes, it was possible to assign the unit cost to every element in the dataset of the road exposure module. Following the protocol's recommendations, the roads with sophisticated accessories were combined with the middle point (quantile 3) between the average to maximum construction cost for each type of road in the Table 20, while roads without accessories (simple roads) were combined with the middle point (quantile 1) between minimum to average cost. It is recommended to create the taxonomy codes in the way that accessories could be identified to make a better fit with the values in the Table 20.

Table 20: Minimum and maximum construction costs per road type (price level: average of the former EU-28, in 2015-euro per km). Adapted from van Ginkel, et al., (2021).

Road type	Default number of lanes	Minimum construction costs	Maximum construction costs
Motorway	1*2	€ 1,750,000	€ 17,500,000
Trunk	1*2	€ 1,250,000	€ 3,750,000
Primary	2*1	€ 1,000,000	€ 3,000,000
Secondary	2*1	€ 500,000	€ 1,500,000
Tertiary	2*1	€ 200,000	€ 600,000
Other	1*1	€ 100,000	€ 300,000

Step 2: apply the correction factors for roads with more (or less) than the default number of lanes

Once the unit construction cost has been assigned to each element (line) in the dataset of the road exposure model, a correction factor was applied, by multiplying it with the construction cost, depending on the number of lanes and type of road that each line represents in the exposure model (see Table 21). The most common case, according with the reference values reported by van Ginkel, et al., (2021), is that each line in the exposure module represents two road lanes. However, depending on the data source, it is possible that one line represents more lanes or even one. For this reason, the protocol has the correction factors given in the Table 21, which must be multiplied for the unit construction cost estimated for each element in the road exposure model.

Table 21: Factors for correcting constructing costs deviating from the default number of lanes per road type. Adapted from van Ginkel, et al., (2021).

Road type/#lanes	1	2	3	4	5	6
Motorway	0.75	1	1.25	1.5	1.75	2
Trunk	0.75	1	1.25	1.5	1.75	2
Primary	0.75	1	1.25	1.5	1.75	2
Secondary	0.75	1	1.25	1.5	1.75	2
Tertiary	0.75	1	1.5	1.75	2	2.25
Other	1	1.25	1.5	1.75	2	2.25

Step 3: curves relative to total construction cost

After the application of the correction factors, the total damage cost for each element in the road exposure model was calculated by associating the water depth provided by the hazard maps and the damage curve (shown in the Table 22) associated to the taxonomy codes.

Table 22: Damage curves as fraction of the construction costs. Adapted from van Ginkel, et al., (2021).

Curve 1 (C1)		Curve 2 (C2)		Curve 3 (C3)		Curve 4 (C4)		Curve 5 (C5)		Curve 6 (C6)	
Motorways and trunk roads						Other roads					
Sophisticated accessories				Simple roads (no accessories)							
Low flow		High flow		Low flow		High flow		Low flow		High flow	
Depth (m)	Damage (fraction)	Depth (m)	Damage (fraction)	Depth (m)	Damage (fraction)	Depth (m)	Damage (fraction)	Depth (m)	Damage (fraction)	Depth (m)	Damage (fraction)
0	0	0	0	0	0	0	0	0	0	0	0
0.5	0.01	0.5	0.02	0.5	0.002	0.5	0.015	0.5	0.015	0.5	0.12
1.0	0.03	1.0	0.06	1.0	0.004	1.0	0.04	1.0	0.025	1.0	0.2
1.5	0.075	1.5	0.1	1.5	0.025	1.5	0.2	1.5	0.03	1.5	0.24
2.0	0.1	2.0	0.12	2.0	0.03	2.0	0.25	2.0	0.035	2.0	0.28
6.0	0.2	6.0	0.22	6.0	0.04	6.0	0.35	6.0	0.05	6.0	0.35

Step 4: correct damage for national GDP per capita

In the final step, it is necessary to correct the calculated damage cost $D_{EU28,2015}$ for the price level in a country in a given year, which can be done as shown in Eq. (1):

$$D_{country,2021} = \frac{GDP_{country,2021}}{GDP_{country,2015}} \cdot \frac{GDP_{country,2015}}{GDP_{EU28,2015}} \cdot D_{EU28,2015} = F1 \cdot F2 \cdot D_{EU28,2015} \quad (1)$$

The values of all variables for Italy and Spain are shown in Table 23. The GDPs per capita were obtained for the years 2015 and 2021 from the Eurostat website[11].

[11] https://ec.europa.eu/eurostat/databrowser/view/sdg_08_10/default/table

Table 23 : Reference GDPs per capita and multiplier factors for Italy, Spain and EU-28, in the years 2015 and 2021 according with the World Bank data.

Country	$GDP_{country,2015}$ €	$GDP_{EU28,2015}$ €	$GDP_{country,2021}$ €	F1	F2
Spain	23,090.00	26,700.00	23,450.00	1.015	0.864
Italy	25,860.00	26,700.00	26,700.00	1.032	0.968

3.2.3. Methodology for the railway network vulnerability

The RAIL vulnerability model for railways was designed to estimate the structural damage at a railway track standard cross-section and the resulting repair costs. The model was empirically derived from the Morava River flood event in 2006 at the Austrian Northern Railway.

A railway track standard cross section consists of the substructure elements, superstructure, catenary and signals. Depending on the water level at exposed track sections, different degrees of structural flood damage can be expected at one (or more) of those elements (Kellermann, et al., 2015). Thus, on order to estimate these flood losses, the RAIL model distinguishes three structural damage classes (Kellermann, et al., 2015), which are described in Table 24 and represented graphically in in Figure 32. In this sense, the model design is slightly different from typical damage functions: first, ranges of water levels are associated to main typologies of flood damage that are known to occur in railway infrastructure, and loss estimates are then assigned to those classes.

Table 24: Description of the damage classes in the Railway Infrastructure Loss (RAIL) model (Kellermann, et al., 2015).

Type	Description
Damage class 1	The track substructure is (partly) impounded, but there is no or only little notable damage.
Damage class 2	The substructure and superstructure of the track section are fully inundated and significant structural damage at least to the substructure must be expected.
Damage class 3	Additional damage to the superstructure, catenary and/or signals must be expected here and, most commonly, the standard cross-section

Figure 32: Damage classes differentiated in the Railway Infrastructure Loss (RAIL) model (Kellermann, et al., 2015). Damage class 1 at left, class 2 at centre and class 3 at right.

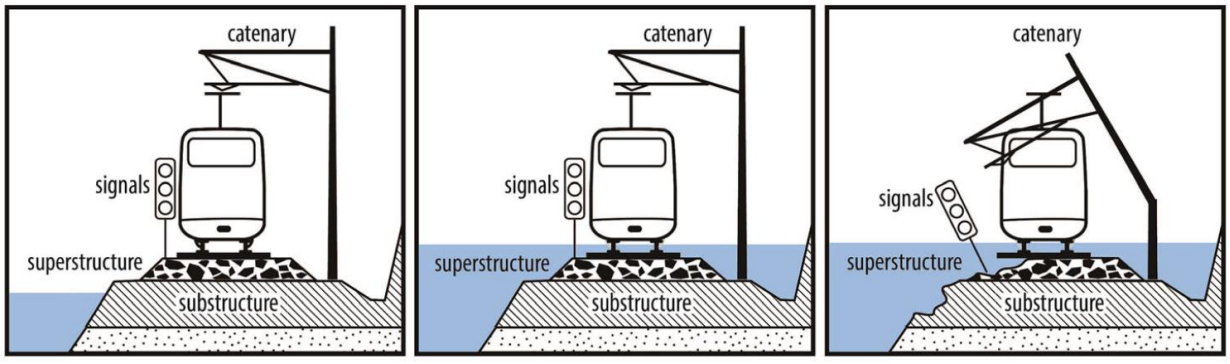

RAIL provides loss estimates in absolute monetary terms. For the estimation of the damage losses due to the repair of damaged track sections, the following standard costs were considered as explained by Kellermann, et al., (2015): (1) costs of loss assessment/ documentation, (2) cost for track cleaning per running meter (rm) and (3) standard cross section repair costs per rm as defined by Austrian railway infrastructure experts. These three cost types were individually combined for each damage class according to the corresponding structural damage pattern. Therefore,

as shown in Table 25, the standard repair costs for a damage class 1 amount to EUR 11,700, the costs for damage class 2 are EUR 135,550 and the costs for damage class 3 total EUR 702,200, whereby all values refer to a 100-metre section of a double-tracked railway line. For single tracked railway lines, these values have to be adapted.

Table 25: - Standard repair costs per 100-metre segment of a double-tracked railway standard cross-section in Austria, 2006 (Kellermann, et al., 2015).

	Damage class 1	Damage class 2	Damage class 3
Cost per 100 m segment	EUR 11,700	EUR 135,550	EUR 702,200

The substructure is the most expensive element of a railway standard cross section and, hence, has a notably high weight within the estimation of repair costs. However, since it is not assured that a full restoration of the substructure is required when a track section is classified as damage class 2, the loss estimates had to be calibrated. Hence, a proportional factor for damage to the substructure in damage class 2 was determined on the basis of the empirical damage data. This approach resulted in a cost calibration factor for damage class 2 amounting to 0.25 (Kellermann, et al., 2016). Considering this, the damage class 3 multiplied by 0.25 results as EUR 175 550, which means that in difference with EUR 135,550 of damage class 2, the remaining 40,000 corresponds to the value of the superstructure.

The repair costs shown in Table 25 were estimated for a 2006 scenario in Austria, so for application to the two scenarios in Spain (destination country), these values were adjusted for the year of 2021. This was done by multiplying the reference damage cost (damage cost of Austria 2006) by two coefficients, first by an adjustment factor between the GDP of the reference year and the current year of the destination country, followed by another adjustment factor between the GDP of the reference country and that of the destination country in the reference year. This is presented in the Eq. (2):

$$D_{Spain,2021} = \frac{GDP_{Spain,2021}}{GDP_{Spain,2006}} * \frac{GDP_{Spain,2006}}{GDP_{Austria,2006}} * D_{Austria,2006} \quad (2)$$

The analysis of the hydraulic impact data performed by the authors of the RAIL model determined that the threshold parameters for differentiating between the 3 types of damage in reference to water depth correspond to 0.2 meters for moving from damage class 1 to damage class 2 and 1.4 meters for moving from damage class 2 to damage class 3, as shown in Figure 33.

Figure 33: Threshold parameters for water level between the damage classes. Extracted from (Kellermann, et al., 2015).

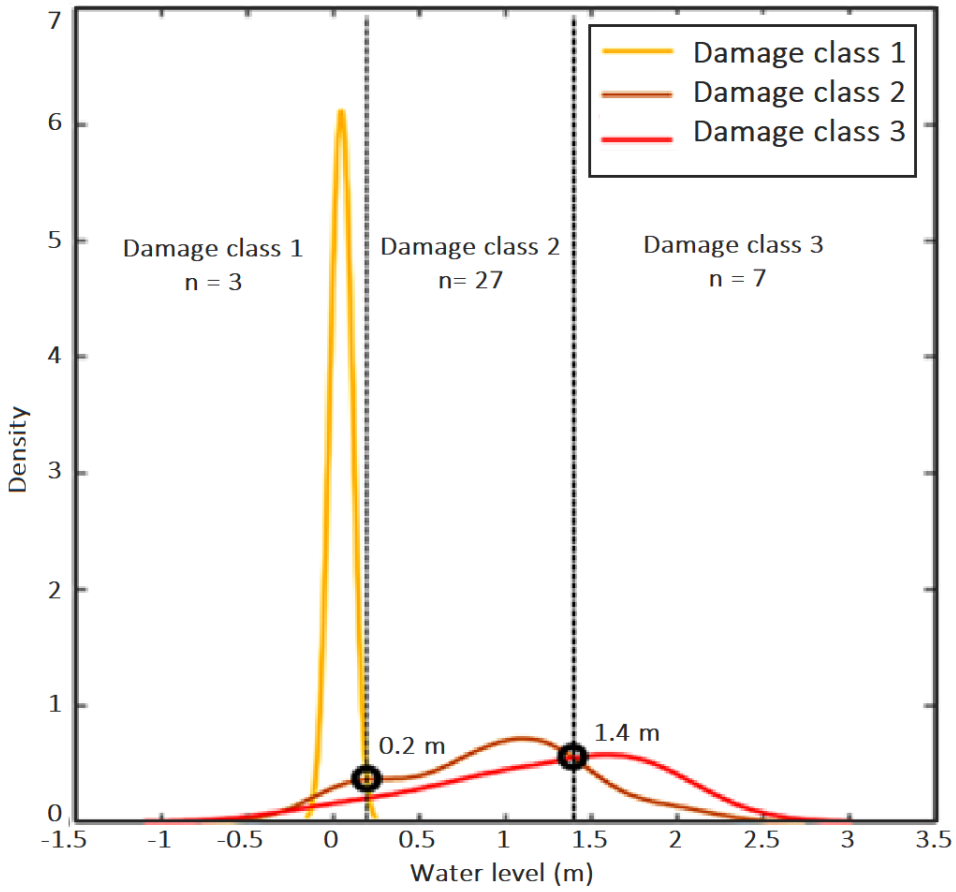

In Kellermann, et al., (2016), the RAIL model was applied in a larger scale scenario in the Mur river basin (Austria) and through a sensitivity analysis by varying 1) the substructure height and 2) the damage class 2 cost calibration factor. As a start, it was considered that although damage class 2 starts at a water height of 0.2 meters, the substructure height is 1 meter high as a reference value according to Rahn (2007), so the damage should be considered at this height. The sensitivity analysis consisted of two variations: a) substructure height of 1.2 meters and damage class 2 cost calibration factor of 0.2, and b) substructure height of 0.8 meters and damage class 2 cost calibration factor of 0.3. This sensitivity exercise serves as a reference to find a calibration point for any scenario in the application of the RAIL model, including the two CCLLs in this study with railway network within the study area, i.e., Oarsoaldea and Vilanova i la Geltrú.

4. CONCLUSION

This report presented the exposure datasets and vulnerability functions that were developed for WP6's three frontrunners CCLLs: Massa, Oarsoaldea, and Vilanova i la Geltrú. Two key types of elements of the built environment were considered in this task: buildings and transportation networks (specifically, road and railway networks). Moreover, a gridded exposure dataset for population was also elaborated. For each component, this document presents a brief contextualization and review of the state of the art, a description of the adopted methodologies and justification for their selection, and the produced outputs. The outputs compose D6.3, which is delivered concurrently with the present report.

The exposure and vulnerability assessments carried out in Task 6.2 and described in this document represent a key milestone in SCORE's WP6 activities, as they will be used to directly inform the subsequent quantitative risk assessments that will be carried out in the context of Task 6.3. Specifically, these modelling components, together with the flood hazard models that will be provided in WP3, will allow computing metrics such as annual average losses, average number of affected persons, loss exceedance probability curve, and economic losses for low probability events for various scenarios. These metrics are expected to contribute to a more informed and effective risk management in the aforementioned CCLLs.

5. REFERENCES

Alfieri, L., L. Feyen, e G. Di Baldassarre. 2016. «Increasing flood risk under climate change: a pan-European assessment of the benefits of four adaptation strategies.» Clim. Change (136): 507–521. doi:10.1007/s10584-016-1641-1.

Alfieri, Lorenzo, Berny Bisselink, Francesco Dottori, Gustavo Naumann, Ad de Roo, Peter Salamon, Klaus Wyser, e Luc Feyen. 2017. «Global projections of river flood risk in a warmer world.» Earth's Future 171-182. doi:10.1002/2016EF000485.

Amadio, M., A. Rita Scorzini, F. Carisi, H.A. Essenfelder, A. Domeneghetti, J. Mysiak, e A. Castellarin. 2019. «Testing empirical and synthetic flood damage models: The case of Italy.» Natural Hazards and Earth System Sciences 19 (3): 661–678. doi:10.5194/nhess-19-661-2019.

Barrington-Leigh, C., e A. Millard-Ball. 2017. «The world's user-generated road map is more than 80% complete.» PLoS ONE (8): 12. doi:10.1371/journal.pone.0180698.

Birkmann, J. 2006. Measuring Vulnerability to Natural Measuring Vulnerability to Natural Resilient Societies. Tokyo, Japan: United Nations.

Bubeck, P., H. de Moel, L.M. Bouwer, e J.C.J.H. Aerts. 2011. «How reliable are projections of future flood damage?» Nat. Hazards Earth Syst. Sci. (11): 3293–3306. doi:10.5194/nhess-11-3293-2011.

Bubeck, P., L. Dillenardt, L. Alfieri, L. Feyen, A.H. Thieken, e P. Kellermann. 2019. «Global warming to increase flood risk on European railways.» Climatic Change (155): 19-36. doi:10.1007/s10584-019-02434-5.

Cammerer, H., A.H. Thieken, e J. Lammel. 2013. «Adaptability and transferability of flood loss functions in residential areas.» Natural Hazards and Earth System Sciences 13 (11): 3063–3081. doi:10.5194/nhess-13-3063-2013.

CAPRA. 2016. Methods in Flood Hazard and Risk Assessment. Washington, DC: International Bank for Reconstruction and Development / The World Bank.

Charles, P. 2007. The Next Catastrophe. Princeton: Princeton University Press.

Chen, K., J. McAneney, R. Blong, R. Leigh, L. Hunter, e C. Magill. 2004. «Defining area at risk and its effect in catastrophe loss estimation: A dasymetric mapping approach.» Applied Geography 24 (2): 97–117. doi:10.1016/j.apgeog.2004.03.005.

Crowley, H., V. Despotaki, D. Rodrigues, V. Silva, D. Toma-Danila, E. Riga, A. Karatzetzou. 2020. «Exposure model for European seismic risk assessment.» Earthquake Spectra 36 (1_suppl): 252–273. doi:10.1177/8755293020919429.

De Bono, A., e M. G. Mora. 2014. «A global exposure model for disaster risk assessment.» International Journal of Disaster Risk Reduction 10 (Part B): 442-451. doi:10.1016/j.ijdrr.2014.05.008.

de Brujin, K., D. wagenaar, K. Slager, M. de Bel, e A. Burzel. 2015. Updated and improved method for flood damage assessment: SSM2015 (version 2). Deltares.

de Moel, H., B. Jongman, H. Kreibich, B. Merz, E. Penning-Rowsell, e P.J. Ward. 2015. «Flood risk assessments at different spatial scales.» Mitig. Adapt. Strateg. Glob. Chang. (20): 865–890. doi:10.1007/s11027-015-9654-z.

de Moel, H., M. van Vliet, e J. C. J. H. Aerts. 2013. «Evaluating the effect of flood damage-reducing measures: a case study of the unembanked area of Rotterdam, the Netherlands.» Regional Environmental Change 14 (3): 895–908. doi:10.1007/s10113-013-0420-z.

Deckers, P., W. Kellens, J. Reyns, W. Vanneuville, e P.D. Maeyer. 2010. "A GIS for flood risk management in Flanders", in Showalter, P.S. and Lu, Y. (Eds). Dordrecht: Springer.

Dell'Acqua, F., P. Gamba, e K. Jaiswal. 2013. «Spatial aspects of building and population exposure data and their implications for global earthquake exposure modeling.» Natural Hazards 68 (3): 1291–1309. doi:10.1007/s11069-012-0241-2.

Dottori, F., R. Figueiredo, M. Martina, D. Molinari, e A.R. Scorzini. 2016. «INSYDE: a synthetic, probabilistic flood damage model based on explicit cost analysis.» Natural Hazards and Earth System Sciences. 16 (12): 2577–2591. doi:10.5194/nhess-16-2577-2016.

FEMA. 2022. National Risk Index Official website of the Department of Homeland Security. 03 12. https://hazards.fema.gov/nri/exposure.

Figueiredo, R., e M. Martina. 2016. «Using open building data in the development of exposure data sets for catastrophe risk modelling.» Natural Hazards and Earth System Sciences 16 (2): 417–429. doi:10.5194/nhess-16-417-2016.

Figueiredo, R., K. Schröter, A. Weiss-Motz, M. L. V. Martina, e H. Kreibich. 2018. «Multi-model ensembles for assessment of flood losses and associated uncertainty.» Natural Hazards and Earth System Sciences (18): 1297–1314. doi:10.5194/nhess-18-1297-2018.

Forzieri, G., A. Bianchi, F.B. e Silva, M.A.M. Herrera, A. Leblois, C. Lavalle, J.C.J.H. Aerts, e L. Feyen. 2018. «Escalating impacts of climate extremes on critical infrastructures in Europe.» Glob Environ Chang (48): 97-107.

Galasso, C., M. Pregnolato, e F. Parisi. 2021. «A Model Taxonomy for Flood Fragility and Vulnerability Assessment of Buildings.» International Journal of Disaster Risk Reduction (53): 101985. doi:10.1016/j.ijdrr.2020.101985.

Gerl, T., H. Kreibich, G. Franco, D. Marechal, e K. Schröter. 2016. «A Review of Flood Loss Models as Basis for Harmonization and Benchmarking.» Plos One 11 (7). doi:10.1371/journal.pone.0159791.

Gil, J., e P. Steinbach. 2008. «From Flood Risk To Indirect Flood Impact: Evaluation Of Street Network Performance For Effective Management, Response And Repair.» WIT Transactions on Ecology and the Environment (10): 335 - 344. doi:10.2495/FRIAR080321.

Habermann, Nadine, e Ralf Hedel. 2018. «Damage functions for transport infrastructure.» International Journal of Disaster Resilience in the Built Environment (Emerald Publishing Limited) 9 (4/5): 420-434. doi:10.1108/IJDRBE-09-2017-0052.

Hirabayashi, Y., R. Mahendran, S. Koirala, L. Konoshima, D. Yamazaki, W. Satoshi, H. Kim, e S. Kanae. 2013. «Global flood risk under climate change.» Nature Clim Change (3): 816–821.

Huizinga, J., H. De Moel, e W. Szewczyk. 2017. Global flood depth-damage functions: Methodology and the database with guidelines. EUR 28552 EN, Luxembourg: Publications Office of the European Union. doi:10.2760/16510.

IPCC. 2014. Climate change 2014: mitigation of climate change. Contribution of working group III to the fifth assessment report of the intergovernmental panel on climate change. United Kingdom and New York: Cambridge.

IPCC. 2007. Fourth Assessment Report: Climate Change 2007 (AR4). IPCC.

Jenelius, E., T. Peterson, e L.-G. Mattsson. 2006. «Importance and exposure in road network vulnerability analysis.» Transportation Research Part A: Policy and Practice 40 (7): 537-560. doi:10.1016/j.tra.2005.11.003.

Kang, J., M. Su, e L. Chang. 2005. «Loss functions and framework for regional flood damage estimation in residential areas.» Journal of Marine Science and Technology 193-199.

Kellermann, P., A. Schöbel, G. Kundela, e A.H. Thieken. 2015. «Estimating flood damage to railway infrastructure – the case study of the March River flood in 2006 at the Austrian Northern Railway.» Nat. Hazards Earth Syst. Sci. (15): 2485–2496.

Kellermann, Patric, Christine Schönberger, e Annegret H. Thieken. 2016. «Large-scale application of the flood damage model Railway Infrastructure Loss (RAIL).» Nat. Hazards Earth Syst. Sci. 16: 2357–2371.

Koks, E.E., J. Rozenberg, C. Zorn, M. Tariverdi, M. Vousdoukas, S.A. Fraser, J.W. Hall, e S. Hallegatte. 2019. «A global multi-hazard risk analysis of road and railway infrastructure assets.» Nat Commun (10): 2677. doi:10.1038/s41467-019-10442-3.

Kreibich, H, K. Piroth, I Seifert, H. Maiwald, U. Kunert, J. Schwarz, B. Merz, e A.H. Thieken. 2009. «Is flow velocity a significant parameter in flood damage modelling?» Nat. Hazards Earth Syst. Sci. (9): 1679–1692. doi:10.5194/nhess-9-1679-2009.

Lummen, N.S., e F. Yamada. 2014. «Implementation of an integrated vulnerability and risk assessment model.» Nat. Hazards (73): 1085–1117. doi:10.1007/s11069-014-1123-6.

Merz, B., H. Kreibich, R. Schwarze, e A. Thieken. 2010. «Review article "Assessment of economic flood damage".» Nat. Hazards Earth Syst. Sci. 10 (8): 1697–1724. doi:10.5194/nhess-10-1697-2010.

Molinari, D., A.R. Scorzini, C. Arrighi, F. Carisi, F. Castelli, A. Domeneghetti, A. Gallazzi. 2020. « Are flood damage models converging to "reality"? Lessons learnt from a blind test.» Natural Hazards and Earth System Sciences 20 (11): 2997–3017.

Papilloud, T., e M. Keiler. 2021. «Vulnerability patterns of road network to extreme floods based on accessibility measures.» Transportation Research Part D (100): 103045.

Paul, N., V. Silva, e D. Amo-Oduro. 2022. «Development of a uniform exposure model for the African continent for use in disaster risk assessment.» Disaster Risk Reduction 71: 102823. doi:10.1016/j.ijdrr.2022.102823.

Peduzzi, P., H. Dao, C. Herold, e F. Mouton. 2009. «Assessing global exposure and vulnerability towards natural hazards: the Disaster Risk Index.» Nat. Hazards Earth Syst. Sci. (9): 1149–1159.

Prahl, B.F., D. Rybski, M. Boettle, e J.P. Kropp. 2016. «Damage functions for climate-related hazards: unification and uncertainty analysis.» Nat. Hazards Earth Syst. Sci. (16): 1189–1203.

Rahn, H. 2007. Eisenbahndämme und Einschnitte, in: Handbuch Eisenbahninfrastruktur. A cura di L. Fendrich. Berlin, Heidelberg: Springer Verlag.

Schröter, K., H. Kreibich, K. Vogel, C. Riggelsen, F. Scherbaum, e B. Merz. 2014. «How useful are complex flood damage models?» Water Resources Research 50 (4): 3378–3395. doi:10.1002/2013WR014396.

Shi, Y., S. Blainey, C. Sun, e P. Jing. 2020. «literature review on accessibility using bibliometric analysis techniques.» J. Transp. Geogr. (87): 102810. doi:10.1016/j.jtrangeo.2020.102810.

Silva, V., H. Crowley, H. Varum, e R. Pinho. 2015. «Seismic risk assessment for mainland Portugal.» Bulletin of Earthquake Engineering 13 (2): 429-457. doi:10.1007/s10518-014-9630-0.

Thieken, A.H., V. Ackermann, F. Elmer, H. Kreibich, B. Kuhlmann, U. Kunert, H. Maiwald. 2009. «Methods for the evaluation of direct and indirect flood losses.» RIMAX Contributions at the 4th International Symposium on Flood Defence. Toronto, Ontario, Canada: ISFD4, 6-8 May 2008.

UNISDR. 2016. Report of the open-ended intergovernmental expert working group on indicators and terminology relating to disaster risk reduction. United Nations General Assembly.

van Ginkel, Kees C.H., Francesco Dottori, Lorenzo Alfieri, Luc Feyen, e Elco E. Koks. 2021. «Flood risk assessment of the European road network.» Nat. Hazards Earth Syst. Sci. (21): 1011–1027. doi:10.5194/nhess-21-1011-2021.

Vanneuville, W., P.D. Maeyer, K. Maeghe, e F. Mostaert. 2003. «Model of the effects of a flood in the Dender catchment, based on a risk methodology.»

Vanneuville, W., R. Gamanya, K.D. Rouck, K. Maeghe, e P.D. Maeyer. 2005. «Development of a flood risk model and applications in the management of hydrographical catchments.»

Verwaest, T., P. Vanpoucke, J. Reyns, K. van der Biest, P. Vanderkimpen, P. Peeters, W. Kellens, e W. Vanneuville. 2008. «Comparison between different flood riskmethodologies.» Action 3B Report.

Winsemius, H.C., L.P.H. Van Beek, B. Jongman, P.J. Ward, e A. Bouwman. 2013. «A framework for global river flood risk assessments.» Hydrol. Earth Syst. Sci. (17): 1871–1892. doi:10.5194/hess-17-1871-2013.